AD-A134 605 GRAIN REFINING AND MICROSTRUCTURAL MODIFICATION DURING SOLIDIFICATION(U) FLORIDA UNIV GAINESVILLE DEPT OF MATERIALS SCIENCE AND ENGINEERING G J ABBASCHIAN 1/1

UNCLASSIFIED OCT 83 TR-2 N00014-81-K-0730 F/G 11/6 NL

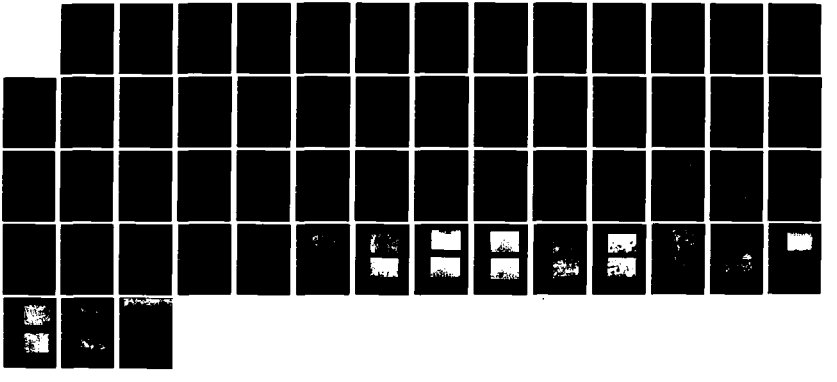

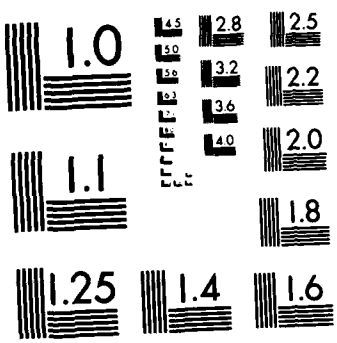

MICROCOPY RESOLUTION TEST CHART
NATIONAL BUREAU OF STANDARDS-1963-A

(12)

Technical Report No. 2
Contract N00014-81-K-0730; NR031-836

GRAIN REFINING AND MICROSTRUCTURAL MODIFICATION DURING SOLIDIFICATION

G. J. Abbaschian
Department of Materials Science and Engineering
University of Florida
Gainesville, FL 32611

20 October 1983

Annual Report for Period 1 September 1982-31 August 1983

OFFICE OF NAVAL RESEARCH
Materials Division
800 N. Quincy Street
Arlington, VA 22217

Unclassified

SECURITY CLASSIFICATION OF THIS PAGE (When Data Entered)

REPORT DOCUMENTATION PAGE	READ INSTRUCTIONS BEFORE COMPLETING FORM
1. REPORT NUMBER	2. GOVT ACCESSION NO. A134605 / 3. RECIPIENT'S CATALOG NUMBER
4. TITLE (and Subtitle) GRAIN REFINING AND MICROSTRUCTURAL MODIFICATION DURING SOLIDIFICATION	5. TYPE OF REPORT & PERIOD COVERED Annual Report September 1982-August 1983 / 6. PERFORMING ORG. REPORT NUMBER
7. AUTHOR(s) G. J. Abbaschian	8. CONTRACT OR GRANT NUMBER(s) N00014-81-K-0730; NR031-836
9. PERFORMING ORGANIZATION NAME AND ADDRESS University of Florida Department of Materials Science & Engineering Gainesville, Florida 32611	10. PROGRAM ELEMENT, PROJECT, TASK AREA & WORK UNIT NUMBERS
11. CONTROLLING OFFICE NAME AND ADDRESS Department of the Navy Materials Division - Office of Naval Research Arlington, Virginia 22217	12. REPORT DATE October 1983 / 13. NUMBER OF PAGES 49
14. MONITORING AGENCY NAME & ADDRESS(if different from Controlling Office)	15. SECURITY CLASS. (of this report) Unclassified / 15a. DECLASSIFICATION/DOWNGRADING SCHEDULE

16. DISTRIBUTION STATEMENT (of this Report)

Approved for public release; distribution unlimited. Reproduction in whole or in part is permitted for any purpose of the United States government.

17. DISTRIBUTION STATEMENT (of the abstract entered in Block 20, if different from Report)

18. SUPPLEMENTARY NOTES

19. KEY WORDS (Continue on reverse side if necessary and identify by block number)

Grain refining, microstructure, solidification, supercooling, phase diagrams, electromagnetic stirring, Cu-Fe alloys, Cu-Nb and Ni-Cr alloys.

20. ABSTRACT (Continue on reverse side if necessary and identify by block number)

This is the second annual report of a three-year research program initiated in the Materials Science and Engineering Department of the University of Florida on September 1, 1981. The objective of the program is to study grain refining and microstructural modification during solidification, as affected by supercooling, solidification rate, and/or inoculation. The report summarizes some of the findings from the

DD FORM 1 JAN 73 1473 EDITION OF 1 NOV 65 IS OBSOLETE S/N 0102-LF-014-6601

Unclassified

SECURITY CLASSIFICATION OF THIS PAGE (When Data Entered)

first year of the program and covers details of the current investigations on the structure and phase transformations in Cr-Ni alloys, the effect of electromagnetic stirring on the structure of Cr-Ni alloys, and grain refining via peritectic transformations in Cu.

The effect of iron and niobium additions on the grain size of copper was studied. The experiments showed that iron is effective in reducing as-cast grain size of copper in concentrations as low as 1.0 percent, and the grain size decreased with increasing the amount of iron. In alloys containing more than the peritectic liquid composition, 2.8 percent, the grain size was found to be insensitive to the iron concentration in the samples solidified in the levitated state but not in samples quenched from the liquid. The preliminary results with niobium additions indicate that no appreciable grain refinement is achieved when the samples are levitated in an inert atmosphere. However, appreciable grain refinement was observed when the samples were melted in a reducing atmosphere.

Research on the solidification of Cr-Ni alloys has led to the observation of various phase transformations in the alloy system. The results indicate that the accepted phase diagram for Cr-Ni, consisting of a eutectic transformation only, is incorrect. The diagram should include a eutectic, a peritectic, and a eutectoid for the decomposition of the periectic phase. It possibly includes another second eutectoid involving an allotropic phase transformation in Cr. The existence of the second eutectoid is not definite yet, and verification experiments are underway.

The effect of electromagnetic stirring on the structure of Cr-Ni alloys has been shown to cause considerable dendrite fragmentation, and consequently grain refinement. The dendrite fragmentation appears to be due mostly to dendrite remelting and coarsening, rather than physical disintegration of the dendrites.

A-1

Technical Report No. 2
Contract N00014-81-K-0730; NR031-836

GRAIN REFINING AND MICROSTRUCTURAL MODIFICATION DURING SOLIDIFICATION

G. J. Abbaschian
Department of Materials Science and Engineering
University of Florida
Gainesville, FL 32611

20 October 1983

Annual Report for Period 1 September 1982-31 August 1983

OFFICE OF NAVAL RESEARCH
Materials Division
800 N. Quincy Street
Arlington, VA 22217

FOREWORD

This research was supported by the Office of Naval Research, Arlington, Virginia, under contract number N00014-81-K-0730. The scientific officer monitoring the program was Dr. Bruce A. MacDonald. Contributions from German Amaya, Joseph A. Patchett, and Robert Schmees are gratefully acknowledged. Special thanks are due to Professor John Hren, Dr. Stanley Bates, and the staff of the Analytical Instrumental Center for their assistance in the microscopy work, and to Miss Torri Jackson for typing the manuscript.

TABLE OF CONTENTS

ABSTRACT

This is the second annual report of a three-year research program initiated in the Materials Science and Engineering Department of the University of Florida on September 1, 1981. The objective of the program is to study grain refining and microstructural modification during solidification, as affected by supercooling, solidification rate, and/or inoculation. The report summarizes some of the findings from the first year of the program and covers details of the current investigations on the structure and phase transformations in Cr-Ni alloys, the effect of electromagnetic stirring on the structure of Cr-Ni alloys, and grain refining via peritectic transformations in Cu.

The effect of iron and niobium additions on the grain size of copper was studied. The experiments showed that iron is effective in reducing as-cast grain size of copper in concentrations as low as 1.0 percent, and the grain size decreased with increasing the amount of iron. In alloys containing more than the peritectic liquid composition, 2.8 percent, the grain size was found to be insensitive to the iron concentration in the samples solidified in the levitated state but not in samples quenched from the liquid. The preliminary results with niobium additions indicate that no appreciable grain refinement is achieved when the samples are levitated in an inert atmosphere. However, appreciable grain refinement was observed when the samples were melted in a reducing atmosphere.

Research on the solidification of Cr-Ni alloys has led to the observation of various phase transformations in the alloy system. The results indicate that the accepted phase diagram for Cr-Ni, consisting of a eutectic

transformation only, is incorrect. The diagram should include a eutectic, a peritectic, and a eutectoid for the decomposition of the periectic phase. It possibly includes another second eutectoid involving an allotropic phase transformation in Cr. The existence of the second eutectoid is not definite yet, and verification experiments are underway.

The effect of electromagnetic stirring on the structure of Cr-Ni alloys has been shown to cause considerable dendrite fragmentation, and consequently grain refinement. The dendrite fragmentation appears to be due mostly to dendrite remelting and coarsening, rather than physical disintegration of the dendrites.

I. INTRODUCTION

The importance of attaining fine grain structures during solidification was outlined in the first annual report (1). It was pointed out that commercial grain refining is generally achieved by way of increased nucleation and/or grain multiplication, via controlling thermal, mechanical, and/or chemical conditions during solidification.

One aim of the present research was to better understand the mechanism(s) of grain refining via peritectic transformation. To achieve this, two binary systems, copper-iron and copper-niobium, were chosen, and the effect of compositional variation and cooling rate on the grain size were investigated, as discussed in Section III-a.

Another aspect of the research was to study the effect of supercooling on the microstructure and solute distribution during solidification of various metals and alloys. It was shown that (1,2) the grain size of high purity nickel decreased continuously as the supercooling was increased from 0 to 305K. At low supercoolings, the grains tended to have non-uniform oblong shapes, while at larger supercooling they tended to become more uniform and equiaxed. When the supercooling was larger than about 200K, twinning and various fine-grained zones, interdispersed among the larger grains, were also observed.

Research on the effect of composition and cooling rate on the structure of Cr-Ni has led to the observation of various microstructures that cannot be explained based on the accepted phase diagram of the system. This has led to the critical examination of the Cr-Ni phase diagram, by using high purity starting materials, and a containerless electromagnetic levitation, melting and solidification technique, as discussed in Section III-b.

The Cr-Ni diagram is important in understanding the characteristics of technologically important alloys such as stainless steels and superalloys, which use both chromium and nickel as primary alloying constituents. There has been much dispute in the literature concerning the construction of the binary diagram. The proposed diagrams include the commonly accepted simple eutectic diagram of Figure 1 (3-9), the eutectic-eutectoid diagram of Figure 2 (10-12), the eutectic-peritectic-2 eutectoid diagram of Figure 3 (13,14), and the eutectic-4 eutectoid diagram of Figure 4 (15-19). A further complication is related to the disputed chromium allotropic transformation (10,12,14). The allotropic transformation has been indicated to be highly sensitive to oxygen content (12).

The major difficulties in studying Cr-Ni phase diagram are due to the intense volatilization at high temperatures, the high stability of chromium oxides, solid state precipitation which may obscure phase transformations, and the effect of impurities and containers. In the present study, experiments were designed to minimize some of these effects, especially those related to oxidation, impurities, and container.

Finally, as discussed in Section III-c, research was performed to investigate the effect of electromagnetic stirring on the microstructure and grain size of Cr-Ni alloys. It is shown that electromagnetic stirring causes dendrite fragmentation, leading to considerable grain refinement.

II. EXPERIMENTAL PROCEDURE

The levitation apparatus used in this study consisted mainly of a levitation coil, a two-color pyrometer, a gas purifying system, and a quenching medium (1). The levitation coil consisted of a copper tube wound to have a gap between the upper and the lower turns, with the upper turns wound in reverse direction to the lower. The coil was powdered by a 450 KC, 10 KW high frequency generator. The temperature of the levitated sample was measured and continuously monitored by the two-color pyrometer. The pyrometer reading was calibrated against the melting points of pure iron, nickel and copper. The accuracy of the temperature measurements is ±10°C below 1700°C.

High purity helium, argon, and/or helium-2% hydrogen was continuously passed through the glass tube surrounding the sample in order to provide cooling and to prevent oxidation. The inert gases were purified by passing through a "gas purifier," which utilizes titanium at 800°C as a "getter." The oxygen content of the purified gas was continuously monitored to be in the range of 10^{-15} ppm. The helium-hydrogen gas mixture was passed through an "oxygen excavenger," which catalytically converts residual oxygen into water, and then through a liquid nitrogen trap.

The samples, each weighing about one gram, were prepared from high purity nickel (99.99 and 99.999%), iron (99.98%), copper (99.99 and 99.999%), and/or chromium (99.95 and 99.9999%). The alloys were prepared in a vacuum arc melting furnace partially back filled with argon. A titanium getter was melted prior to melting of the samples.

A sample, as prepared, was lowered into the levitation coil using a nickel wire which was pulled out of the field as soon as the solid sample

levitated. The gas flow and the power input to the coil were adjusted to melt and superheat the sample by about 300K. In order to measure the maximum attainable supercooling, the sample was then cooled at a rate of 5-30 KS^{-1} until nucleation and recalescence took place. After recording the nucleation temperature, the sample was reheated, and the procedure was repeated several times. The sample was finally cooled to a desired temperature where it was allowed to solidify in the levitated state or to fall into the water bath placed beneath the levitation chamber.

III. RESULTS AND DISCUSSION

(a) Grain refining in copper

To study the mechanism of grain refining via peritectic transformation in Cu-Fe and Cu-Nb*, two processing procedures were followed: One involved solidifying the samples in the levitated state, followed by quenching at 1000°C in water. The second procedure consisted of quenching the samples from their liquidus temperatures in water. The Cu-Fe samples were processed in Ar and He atmosphere. For Cu-Nb alloys, some samples were levitated in a hydrogen reducing atmosphere, while others were levitated in the inert gases.

The average grain size versus iron content of samples solidified in the levitated state and subsequently quenched at 1000°C in water is shown in Figure 5, and summarized in Table 1. The addition of iron promotes

*See footnote on page 10.

considerable grain refinement in copper. The extent of the refinement increases with increasing the iron content until about 2.8% Fe, which corresponds to the composition of the peritectic liquid. Beyond this composition, called hyperperitectic regi ⁻, the grain size is not affected appreciably by the iron content.

The grain size of samples quenched from their corresponding liquidus temperatures also showed considerable refinement by the addition of iron, as shown in Figure 6. However, in contrast with the samples solidified while levitated, the grain size continued to decrease in the hyperperitectic regions. The grain size data for the two sets of experiments are compared in Figure 7.

Another method of evaluating the effectiveness of iron as a grain refiner for copper is to look at the degree of supercooling attainable prior to nucleation of the primary phase. From our work and those of others (21,22), pure copper can readily be supercooled in excess of 200°C. In a few cases, it was possible to supercool in excess of 400°C, which corresponds to approximately 0.30 T_m. This is the largest amount of supercooling yet reported for copper. Upon the addition of iron, the ability to supercool the liquid was sharply reduced. For example, a composition of one weight percent iron the maximum supercooling observed was 100°C. As the iron content increased, the amount of supercooling dropped off considerably. Beyond 1.5 percent iron, no appreciable supercooling was observed.

The formation of primary gamma iron was observed at a composition of 2.8±0.05 weight percent iron, which corresponds to that of the peritectic liquid. For compositions close to the peritectic liquid, the grain size shows

a wide scatter. Figure 8 shows two samples having iron concentration of about 2.8%, and solidified under similar conditions but with different grain sizes. The range of mean grain sizes falls outside the confidence intervals for the individual samples. On the hypoperitectic side the grain size variation started at 2.73 percent iron and beyond 2.9 percent iron the data followed the trends in the hyperperitectic region.

In the hyperperitectic region the grain size of the samples solidified in the levitated state was found to be insensitive to the iron concentration as indicated in Figure 5. This can also be seen from the photomicrographs shown in Figure 9 for two samples containing 3.27 percent and 7.46 percent iron. In spite of the large difference in iron concentration, the average grain size is the same in both samples.

As the iron content is increased, the size and number of the iron dendrites increase, as would be expected from the phase diagram. At lower iron concentrations, the iron dendrites are small with only a few side branches. At larger concentrations, however, the dendrites have a well developed dendritic structure consisting of numerous secondary, and in some cases, tertiary arms. These observations are due to the fact that at small iron concentrations the temperature difference between the iron liquidus and the peritectic temperature is small, allowing only a limited time for dendrite growth and coarsening.

The microstructures of two hypoperitectic alloys quenched when fully liquid are illustrated in Figure 10. In the hypoperiectic region, the grain size of the water quenched alloys was not appreciably different from that of the slowly solidified samples (See Figure 7). However, when the recorded mean

values are considered, the grain size of the quenched samples is slightly larger than the mean grain size for the alloys solidified in the levitated state. The data clearly indicates the benefitial grain refining effect of electromagnetic stirring as discussed in more detail later.

The sharp discontinuity in the grain size, which was observed during the transition from hypo- to hyperperitectic compositions in samples solidified in the levitated state, was absent in the quenched data. Instead, the data shows approximately continuous progression to smaller grain sizes as the hyperperitectic region is reached. Within the hyperperitectic region, the grain size continues to decrease as the amount of iron is increased. This can be seen by comparing the structures of the three samples shown in Figure 11.

As a result of rapid solidification in water, the size of the iron primaries decreases and their distribution becomes more uniform. The distinctive morphology of the iron appears to become less dendritic . To investigate the morphology of the iron phase in more detail, the samples were etched in concentrated nitric acid. The nitric acid preferentially dissolved the iron phase, leaving the surrounding copper matrix relatively unaffected. The etched samples were examined in a scanning electron microscope. The results indicated that despite changes in the cooling rate, iron maintains a dendritic morphology. For the sample solidified in the levitated state, some solid state precipitation of iron was also seen in the copper matrix. The precipitates were estimated to be approximately 0.4 microns in diameter. The sample quenched from the liquidus showed no precipitates, indicating that the copper matrix is a supersaturated alpha solid solution.

In the copper-niobium system, composition of the peritectic liquid is at approximately 0.10 weight percent niobium, see Figure 12.* The grain size measurement of various copper-niobium alloys are summarized in Table 2. As was the case with the copper-iron alloys, the samples were either quenched from their liquidus or allowed to solidify in this levitated state and subsequently quenched from 1000°C. In addition, some samples were processed in a hydrogen atmosphere while others were processed in an inert gas.

In all the copper-niobium samples, a high temperature thermal arrest was observed several hundred degrees above the equilibrium liquidus. The thermal arrest was around 1600°C and varied by as much as 100°C from sample to sample. At this temperature small solid patches formed on the surface of the sample, and subsequently agglomerated. These patches, which were presumed to be oxides or slag, would disappear when the sample was superheated about 700°C. Depending on the presence or absence of hydrogen in the coolant gas, the microstructures of the samples were found to fall into two categories as discussed below.

In samples for which hydrogen was not used, interdendritic precipitates in addition to the primary niobium phase were also observed, as shown in Figure 13 for a sample containing 0.47% niobium quenched from the liquidus temperature. The grain size of these samples were generally large and unaffected by the cooling rate. This can be seen by comparing Figure 13 and 14. The sample in the latter figure contains 0.44 percent niobium, and was

*A more recent compilation of Cu-Nb phase diagram (20) indicates that the transformation at the Cu-rich side of the diagram is probably a eutectic, rather than a peritectic. At the present, we are conducting our own experiments to check the two diagrams.

solidifed while levitated. However, as the cooling rate increased, the primary phase became less dendritic and more "blocky" in morphology. When the samples were processed with hydrogen, the structure contained fine-equiaxed grians, as shown in Figure 15 for a 5.18% niobium sample. In general the primary phase in these samples was distributed uniformly and no interdendritic precipitates were observed.

Discussion of Cu-Fe and Cu-Nb results

In the hypoperitectic region, the grain refinement mechanisms could be explained based on the "P" factor (23) or the nucleation entropy criteria (24). The absence of a primary phase precludes the effects of inoculants or the peritectic reaction. The calculated values of the nucleation entropy and the P factor are given in Table 3. Larger values of P and the entropy indicate a greater tendency towards grain refinement. According to the P parameter, it would be expected that the niobium would have a considerably greater grain refining effect than the iron. However, the nucleation entropy, for the two systems are similar indicating that the elements would have similar effect on grain refining of copper.

In the hyperperitectic region, the grain refinement could possibly be due to the growth restrictive nature of the peritectic transformation and the presence of the primary phase acting as an inoculant. One of the proposed criterion for grain refinement is the degree of mismatch between the solid particles and the bulk solid phase. The lattice disregistries for copper nucleating on iron and niobium substrates are summarized in Table 3. The degree of mismatch was found to be the least for copper-iron alloys.

For the hyperperitectic copper-iron alloys, no supercooling of either the primary iron phase or the secondary copper phase was observed. This is in contrast with copper-niobium alloys where a supercooling of approximately 10°C was observed prior to the nucleation of the copper at the peritectic temperature. The supercooling might represent a measure of the driving force necessary for the nucleation of the copper on niobium, indicating that niobium is not as effective as iron. This observation is in agreement with that predicted from the lattice disregistry of Table 4.

One important factor that has not yet been discussed is the effect of the fluid flow induced by the electromagnetic field on the structure. The magnitude of the induced fluid flow can readily be appreciated by observing the rapid movement of solid particles on the surface of a molten sample. The fluid flow could have two possible effects: (1) dendrite fragmentation and/or remelting, and (2) enhanced coarsing and agglomeration especially in the hyperperitectic region. The first effect will cause grain refinement while the second will have the opposite effect. The relative importance of these two would depend on the alloy composition as well as the flow conditions.

Considering first the hypoperitectic alloys, the grain size of the copper-iron alloys did not change between the samples solidified in the levitated state and those quenched from their liquidus. In some cases, the mean grain size actually increased when quenched from the liquidus. Alloys solidified in the levitated state were in the electromagnetic field throughout solidification while alloys quenched from their liquidus solidified outside of the field. Therefore, for the former samples the grain refinement may have been due to the addition of iron as well as the induced fluid flow. For the

quenched samples, however, the effect of electromagnetic stirring was diminished during solidification and the grain refinement was due to the iron additions and cooling rate.

In the hyperperitectic region, the increased fluid flow caused appreciable coarsing and agglomeration of the primary phase particles. It was observed that the primary particles tended to collect on the surface, and in the course of cooling through the solid plus liquid region, the particles grew and coalesced. Because of the agglomeration, the effectiveness of the primary phase to grain refine copper was reduced. This phenomenon is similar to the commonly observed fading phenomenon, as a result of which the effectiveness of the inoculants is found to diminish as the metal is held in the liquid state. For conventional casting processes, the fading process occurs over a period of minutes. In the case of electromagnetic levitation, the increased fluid flow enhances the process appreciably.

b. Structure of Cr-Ni Alloys

In order to check for the existence of allotropic phase transformation in pure chromium, 14 samples with 99.95% purity were levitation melted, and thermal data were obtained during cooling of the samples. The samples were levitated in an argon atmosphere. The oxygen pressure in the gas stream was monitored to be around 10^{-15} ppm. Three of these samples showed two thermal arrests; one at 1880, and another one at 1780°C.* The remaining samples

*It should be noted that since the two-color pyrometer was calibrated up to 1700°C, the absolute values of these temperatures might not be accurate. Below 1700°C the accuracy of the measurements is ± 10°C.

showed a single thermal arrest at 1880°C. Supercooling, at both thermal arrests were also noted. The maximum supercooling was about 150°C for the liquid, and about 180°C at the second thermal arrest.

The first arrest corresponds to the normal melting point of chromium. It is possible that the second thermal arrest is due to some type of phase transformation in Cr. However, it is not clear yet why the transformation did not happen in the other samples. More experiments are being conducted by using 99.9999% pure chromium samples.

To study phase transformation in Cr-Ni alloys, five series of alloys were levitated and quenched at various temperatures. The compositions of the alloys were 80/20, 70/30, 65/35, 60/40, and 50/50 weight percent Cr/Ni. Each sample was melted and solidified several times in the levitated state and the cooling curves were obtained prior to the final quenching cycle.

The cooling curves showed various thermal arrests which were not consistent with the simple eutectic diagram shown in Figure 1. For example, the alloy 60/40 showed four clear thermal arrests at about 1490, 1412, 1343, and 1275°C, see Figure 16. An additional thermal arrest at 1200°C was noted for this alloy in a few cases, but more experiments are being conducted to verify it. The first thermal arrest, at 1490°C, corresponds to the liquidus temperature of the alloy, as noted by the appearance of solid patches on the sample.

The microstructure of the as-quenched samples also showed various features that are not consistent with the simple eutectic diagram. For example, the structure of a 70/30 sample that was quenched from the solid + liquid range at 1400°C is shown in Figure 17. Three regions can be clearly

identified in the Figure; the primary dendrites, etched white, is surrounded by a darker region, which is followed by the interdendritic region. The solidification structure, shown at a higher magnification in Figure 18 is similar to those observed during normal cooling (non-equilibrium) through a peritectic transformation followed by a eutectic transformation. Therefore, the solidification structure of the alloy can be explained based on the phase diagram of Yukawa et al. (shown in Figure 3). The primary dendrites is the chromium phase that undergoes a peritectic reaction to form a second phase, called "σ",* which begins to grow and surround the primary dendrites. When the second phase covers the primary phase, the solidification continues through the σ + L region, and the final liquid to solidify is that of the eutectic. Figure 18 also shows that the second phase has gone through a solid state decomposition, as discussed in more detail later.

The photomicrographs of Figures 19 and 20 show the structure of a 70/30 sample quenched after complete solidification at 908°C. The decomposition of the second phase can also be seen in the Figures.

The solid state decomposition of the second phase generally appeared in three morphologies: (1) in the form of Widmanstäten plates, (2) in the form of a basket-weave pattern, and (3) in the form of blocky precipitates. Figures 21 shows the Widmanstäten structure in a 60/40 alloy that was quenched at 870°C. The basket-weave structure is shown in Figure 22 for a 65/35 sample that was quenched at 1412°C. SEM photo micrographs of Figure 23 show a mixture of Widmanstäten and blocky type structures. In samples which were

*X-ray measurements are being conducted to identify the structure of the second phase.

solidified in the levitated state, a lamellar type morphology was also observed, as shown in Figure 24 for a 60/40 sample.

Summary of Cr-Ni experiments

Three samples of 99.95% purity chromium, out of 14 samples tested, have shown a second thermal arrest around 1780°C, which is about 100°C below the melting point of Cr. Whether the thermal arrest is due to an allotropic phase transformation in Cr, or it is due to other factors is currently being investigated.

The experiments with Cr-Ni alloys indicate that the simple eutectic diagram shown in Figure 1 is probably incorrect. The structures and thermal data clearly indicate a peritectic transformation around 1410, and a eutectic around 1345°C. The peritectic phase decomposes by a eutectoid type transformation, probably around 1275°C, to a two-phase structure. These findings are qualitatively consistent with the diagram proposed by Yukawa et al. (13). A second eutectoid might also be present, which is currently being investigated.

The solid state transformation(s) may result in the formation of the Widmanstäten, the basket-weave, blocky, and/or lamellar type morphologies. The nature of the transformations is not clear yet, and more experiments are being conducted by utilizing X-ray and microhardness techniques.

c. Effect of Elctromagnetic Stirring on the Structure of Ni-Cr alloys

The effect of electromagnetic stirring on the structure of Cr-Ni alloys was studied by quenching levitated samples at various temperatures as described below. In the first set of experiments, the samples were quenched when fully liquid or with a supercooling below the liquidus temperature but before nucleation of the primary phase. In the second set, the samples were quenched after nucleation of the primary phase, but prior to nucleation of the second phase. In the third set, the samples were quenched as soon as the solidification was complete. The as-solidified microstructures of 60 Cr-40 Ni and 80 Cr-20 Ni samples solidified under these conditions are discussed below.

The structure of a 60 Cr-40 Ni samples quenched when fully liquid, as shown in Figure 25, consisted of conventionally shaped chromium dendrites with secondary and in some cases tertiary arms. When the sample was quenched just after nucleation of the primary phase, the structure consisted of coarser but detached chromium dendrites, as shown in Figure 26. At higher magnifications, as shown in Figure 27, evidence of coarsening and dendrite remelting can be observed by the necking at the roots of the dendrite arms. Figure 28 shows the structure of a sample which had completely solidified in the levitated state prior to quenching. The cooling rate during solidification was about 30 K/sec. The structure consists of completely detached dendrite arms. Considerable agglomeration and coarsening has occurred within the structure. It should be noted that since each dendritic element represents a grain, considerable grain refinement has taken place.

The structure of 80 Cr-20 Ni alloys quenched while liquid, consisted of conventional chromium dendritic morphology. An example of the dendritic morphology is shown in Figure 29 where the sub-grain structure and grain boundaries can also be observed. Figure 30 shows the disintegration of the dendritic morphology in a sample which was quenched after complete solidification in the levitated state. The structure consists of spherical chromium dendrite elements.

The microstructures shown in Figures 25-30 indicate that electromagnetic stirring causes considerable dendrite fragmentation and grain refinement. The mechanism of dendrite fragementation appears to be mostly due to remelting and enchanced coarsening, rather than physical breakage of the dendrite arms. The photomicrograph in Figure 27 indicates necking at the root of the dendrite arms, which is caused by fluid flow or thermal fluctuations. It should be noted that the coarsening observed in Figures 26 and 28 may have been aided by the electromagnetic heating since the power input to the coil had to be maintained in order to keep the samples levitated.

IV. REFERENCES

1. G.J. Abbaschian, "Grain Refining and Microstructural Modification during Solidification," First Annual Report, October 15, 1982, ONR Contract No. N00014-81-K-0730, prepared for the Office of Naval Research, Arlington, VA.

2. G.E. Amaya, J.A. Patchett, and G.J. Abbaschian, "Grain Refining in Cr, Ni and Cr-Ni Alloys," in Grain Refinement in Castings and Welds, p. 51, edited by G.J. Abbaschian and S.A. David, Conference Proceedings, TMS-AIME, 1982.

3. C.H.M. Jenkins, E.H. Bucknal, C.R. Austin, and G.A. Mellor, J. Iron Steel Inst., 1937, vol. 136, p. 193.

4. R.O. Williams, "Nature of the Ni-Cr System," Journal of Metals, Trans. AIME, October 1957, p. 1257-1260.

5. C.J. Bechtoldt and H.C. Vacher,"Redetermination of the Chromium and Nickel Solvuses in the Chromium-Nickel System," Trans. of the Metallurgical Society of AIME, February 1961, vol. 221, p. 14-18.

6. R.F. Smart and F.G. Haynes, "Some Observations on the Chromium-Nickel System," Journal of the Institute of Metals, 1962-63, vol. 91, p. 153-157.

7. A. Taylor and R. Floyd, J. Inst. Metals, 1951, vol. 80, p. 577.

8. C.H. Bain, Trans. AIME, 1923, vol. 68, p. 625.

9. W.C. Phebus and F.C. Blake, Physical Review, 1925, vol. 25, p.107.

10. D.S. Bloom and N.J. Grant, Journal of Metals, November, 1951, vol. 191, p. 1009-1014.

11. C. Stein and N.J. Grant, "Chromium-Rich Portion of the Chromium-Nickel phase Diagram," Journal of Metals, Trans. AIME, January 1955, p. 127-134.

12. E.P. Abrahamson and N.J. Grant, "Beta Chromium," Journal of Metals, Trans. AIME, August 1956, p.975-977.

13. N. Yukawa, M. Hida, T. Imura, M. Kawamura, and Y. Mizuno, "Structure of Chromium-Rich Cr-Ni, Cr-Fe, Cr-Co, and Cr-Ni-Fe Alloy Particles Made by Evaporation in Argon," Met. Trans., April 1972, vol. 3, p. 887-895.

14. K. Kimoto and I. Nishida, "An Electron Diffraction Study on the Crystal Structure of a new Modification of Chromium," Journal of the Physical Society of Japan, March 1967, vol. 22, no. 3, p. 744-756.

15. A.T. Grig or'ev et al., "Polymorphic Transformations of Chromium in alloys with Tantalum," Russian Journal of Inorganic Chemistry, November 1960, vol. 5, no. 11, p. 1225-1278.

16. A.T. Grigor'ev et al., "Polymorphic Changes Undergone by Chromium in Chromium-Tantalum Alloys," Russian Journal of Inorganic Chemistry, September 1959, vol. 4, no. 11, p. 984.

17. A.T. Grigor' ev et al., "Polymorphic Changes in Chromium: Diagram of the Chromium-Nickel System in the Chromium-Rich Region," Russian Journal of Inorganic Chemistry, May 1961, vol. 6, no. 5, 639-641.

18. A.T. Grigor' ev et al., "High Temperature Modification in the Chromium-Iron System at Compositions Rich in Chromium," September 1960, vol. 5, no. 9, p. 1036.

19. A.T. Grigor' ev et al., "Chromium-Iron Nickel Alloys," Russian Journal of Inorganic Chemistry, November 1963, vol. 8, no. 11, p. 1342-1344.

20. Bulletin of Alloy Phase diagrams, 2, no. 4, (March 1982), 455.

21. B.L. Jones and G.M. Weston, J. Aust. Inst. of Metals, 15 (1970), 157.

22. R.T. Southin and G.M. Weston, J. Aust. Inst. of Metals, 19 (1974), 93.

23. L.A. Tarshis, J.L. Walker, and J.W. Rutter, Can. J. Phys., 31 (1953), 15.

24. W.V. Youdelis, Metal Sci., 9 (1975), 464.

25. Metals Handbook, Eighth Edition, vol. 8, p. 281.

Table 1

Summary of Grain Size Measurements for
Copper-Iron Alloys

Sample Designation	Concentration of Fe, wt. %	Quenching temp., °C	Grain size,		mm
Fe-Cu A10	0.72	1000	0.21	±	.09
Fe-Cu A61	1.65	1000	0.20	±	.04
Fe-Cu A15	2.14	1000	0.11	±	.04
Fe-Cu A25	2.67	1000	0.12	±	.04
Fe-Cu A4	2.72	1050	0.052	±	.008
Fe-Cu B9	3.80	1000	0.22	±	.08
Fe-Cu B1	2.81	1000	0.11	±	.04
Fe-Cu A41	2.86	1000	0.042	±	.01
Fe-Cu A13	2.88	1000	0.076	±	.013
Fe-Cu A32	3.27	900	0.073	±	.026
Fe-Cu A48	3.35	1000	0.071	±	.02
Fe-Cu A39	7.46	1000	0.072	±	.015
Fe-Cu A57	0.57	1085	0.033	±	.17
Fe-Cu A60	2.05	1090	0.13	±	.05
Fe-Cu B3	2.80	1100	0.74	±	.02
Fe-Cu B4	2.84	1115	0.050	±	.01
Fe-Cu A44	3.04	1150	0.035	±	.008
Fe-Cu B5	3.08	1130	0.032	±	.01
Fe-Cu A20	3.12	1150	0.021	±	.004
Fe-Cu B6	3.20	1124	0.032	±	.007
Fe-Cu A47	3.42	1185	0.037	±	.007
Fe-Cu B7	3.67	1250	0.030	±	.008
Fe-Cu A50	4.06	1265	0.022	±	.008

Table 2

Summary of Grain Size Measurements for
Copper-Niobium Alloys

Sample (Designation)	Concentration of Nb wt.	Quench Temp.	Gas Phase	Grain Size mm
Cu-Nb 16	0.04	1370	He + H_2	.13 ± .05
Cu-Nb 24	5.18	1521	He + H_2	.028 ± .004
Cu-Nb 7	0.44	1000	He	.23 ± 16
Cu-Nb 9	0.47	1613	He	.30 ± 12
Cu-Nb 5	0.43	1000	He	.10 ± 02[a]

[a]The sample contained a mixture of large and fine grains. The grain size determination was done on finer grains only.

Table 3

A comparison of the "P" Parameter, the Nucleation Entropy, and Lattice Mismatch for the Cu-Nb, and Cu-Fe systems

	at "P" 0.1% solute	Nucleation Entropy	% Mismatch with Cu
Cu-Nb*	5.6	-4.527	14.5
Cu-Fe	0.12	-4.427	0.8

*The calculation of the "P" parameter is based on the peritectic phase diagram of Figure 12. A different value will result if the recently proposed diagram of Ref.20 is used.

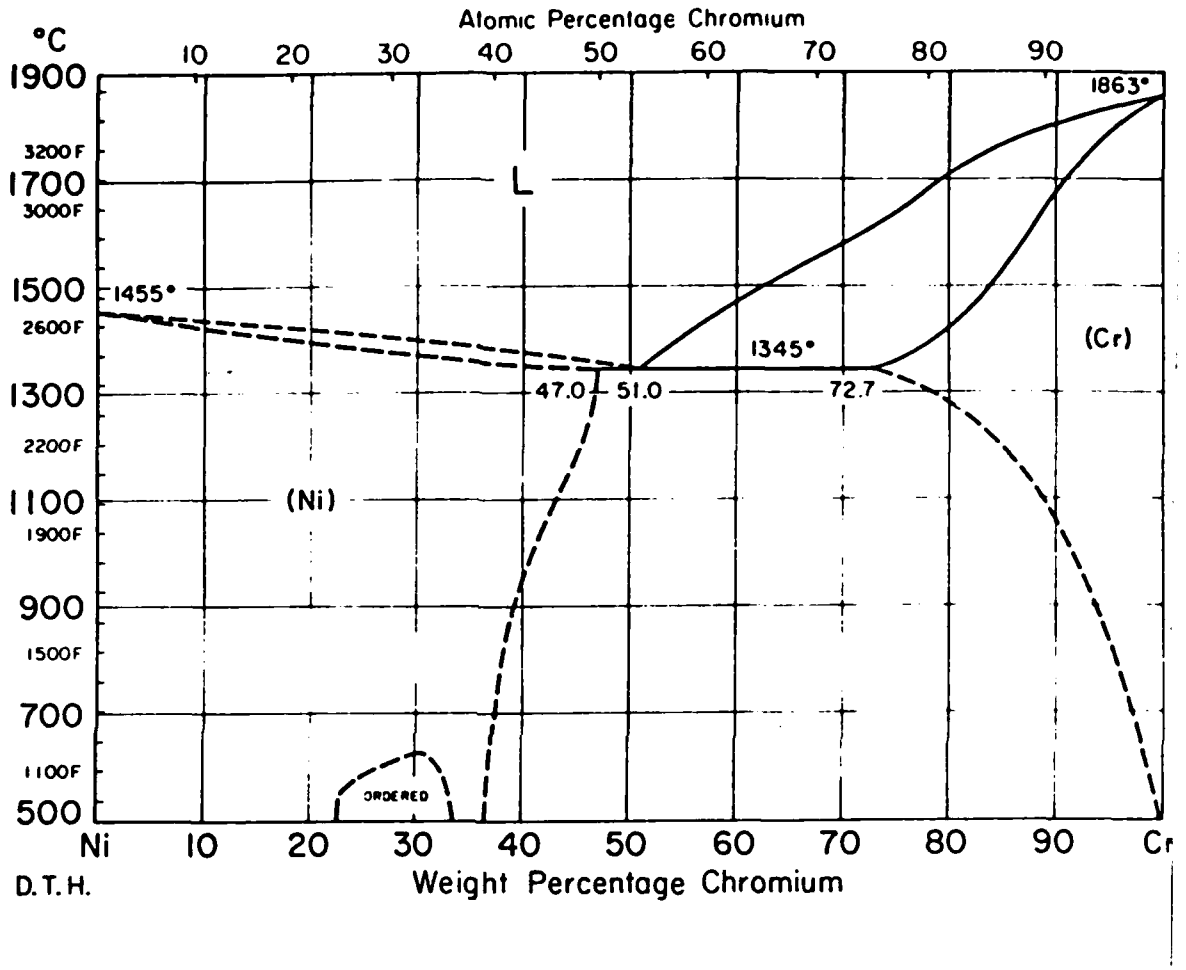

Figure 1. The commonly accepted Cr-Ni phase diagram (Ref. 25).

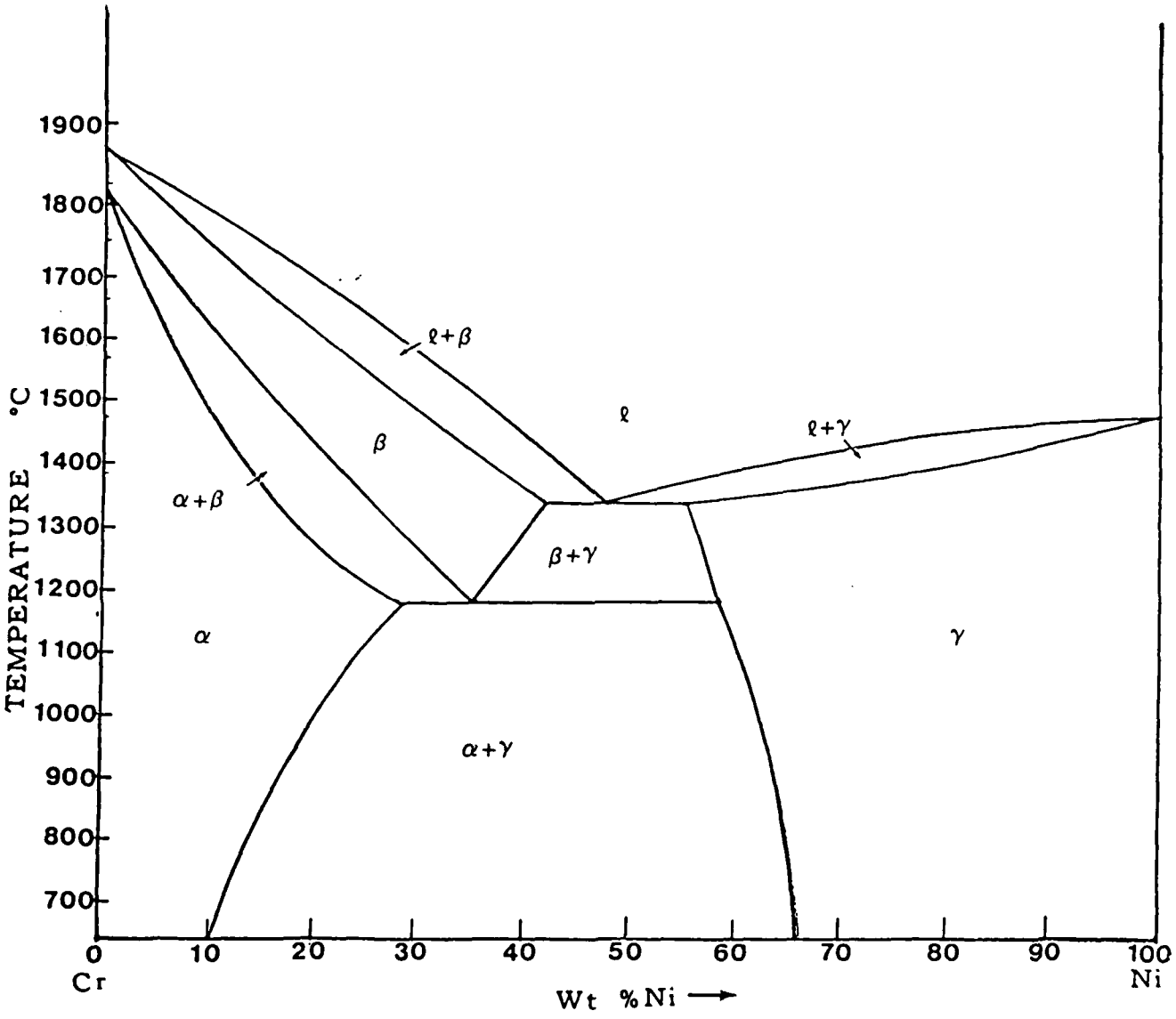

Figure 2. Cr-Ni phase diagram involving a eutectic and a eutectoid (10-12).

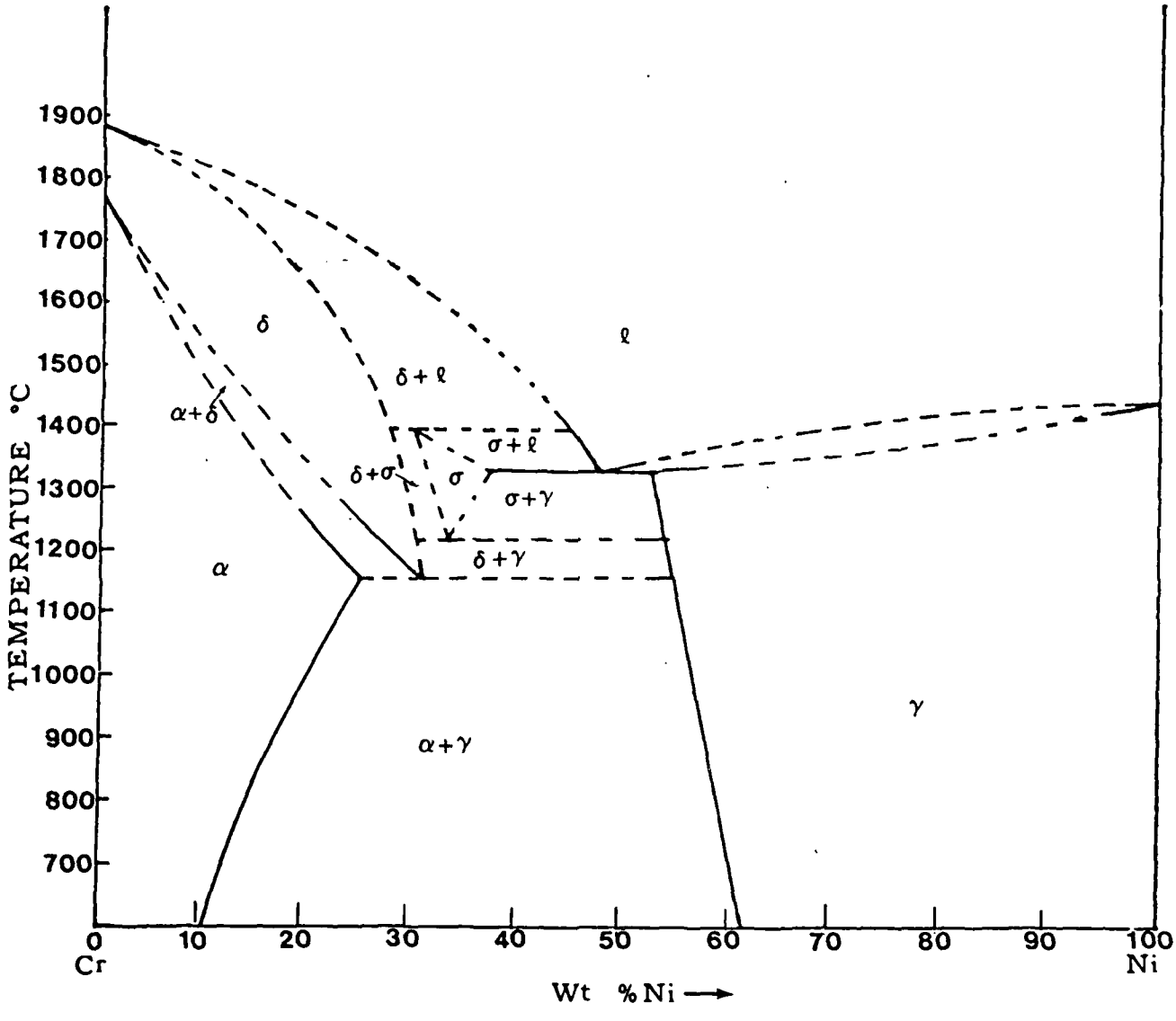

Figure 3. Cr-Ni phase diagram proposed by Yukawa et al (13, 14).

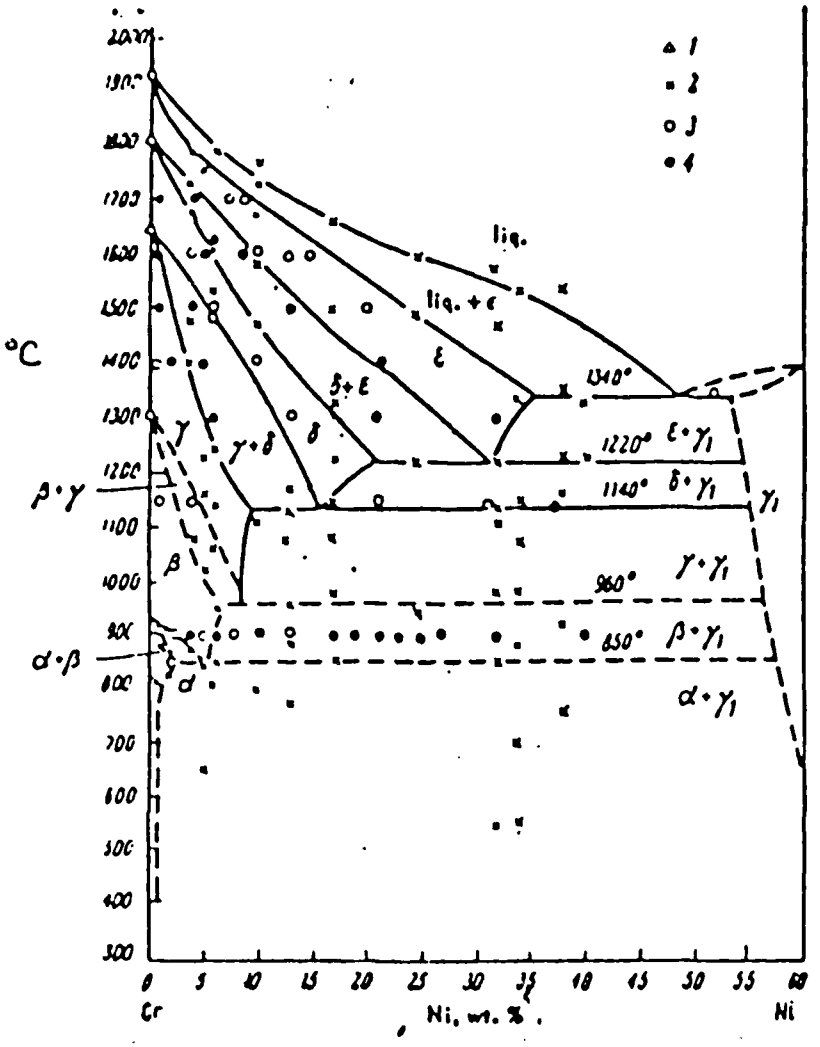

Figure 4. Equilibrium diagram of the chromium-nickel system: 1) polymorphic transformation; 2) thermal analysis; 3) single phase; 4) two phases (15-19).

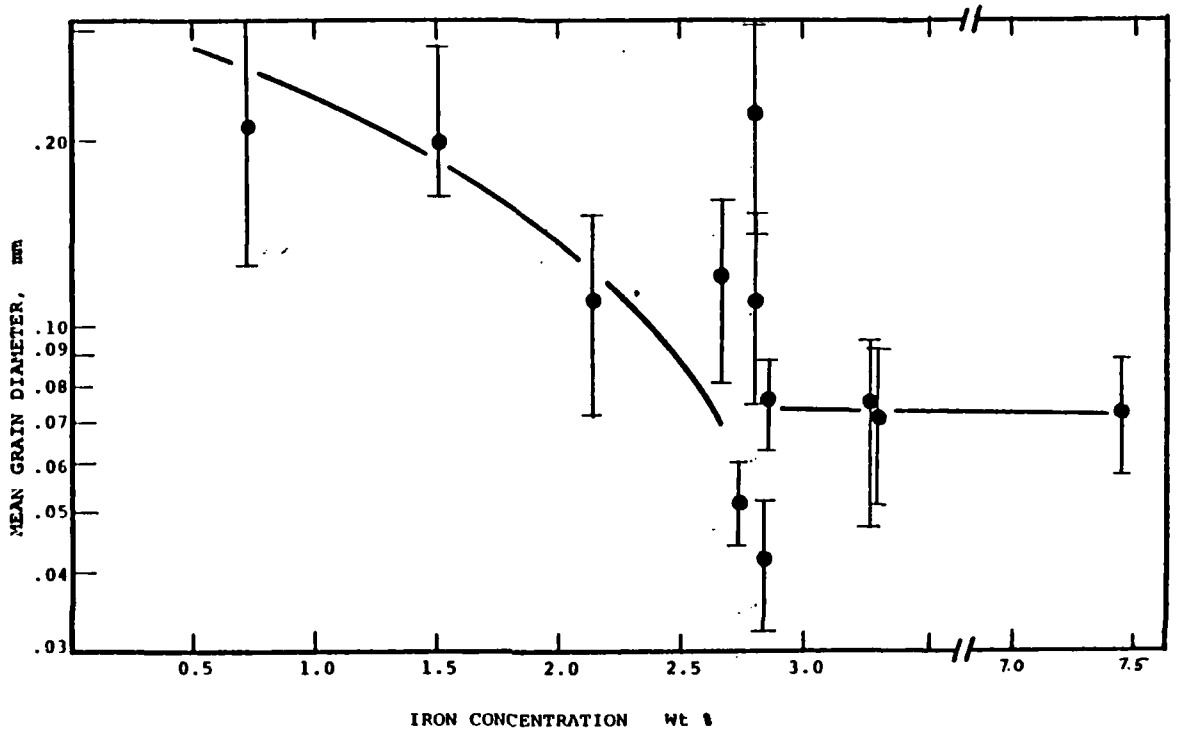

Figure 5. Mean Grain size vs iron content for copper-iron alloys solidified while levitated and quenched in water from 1000°C.

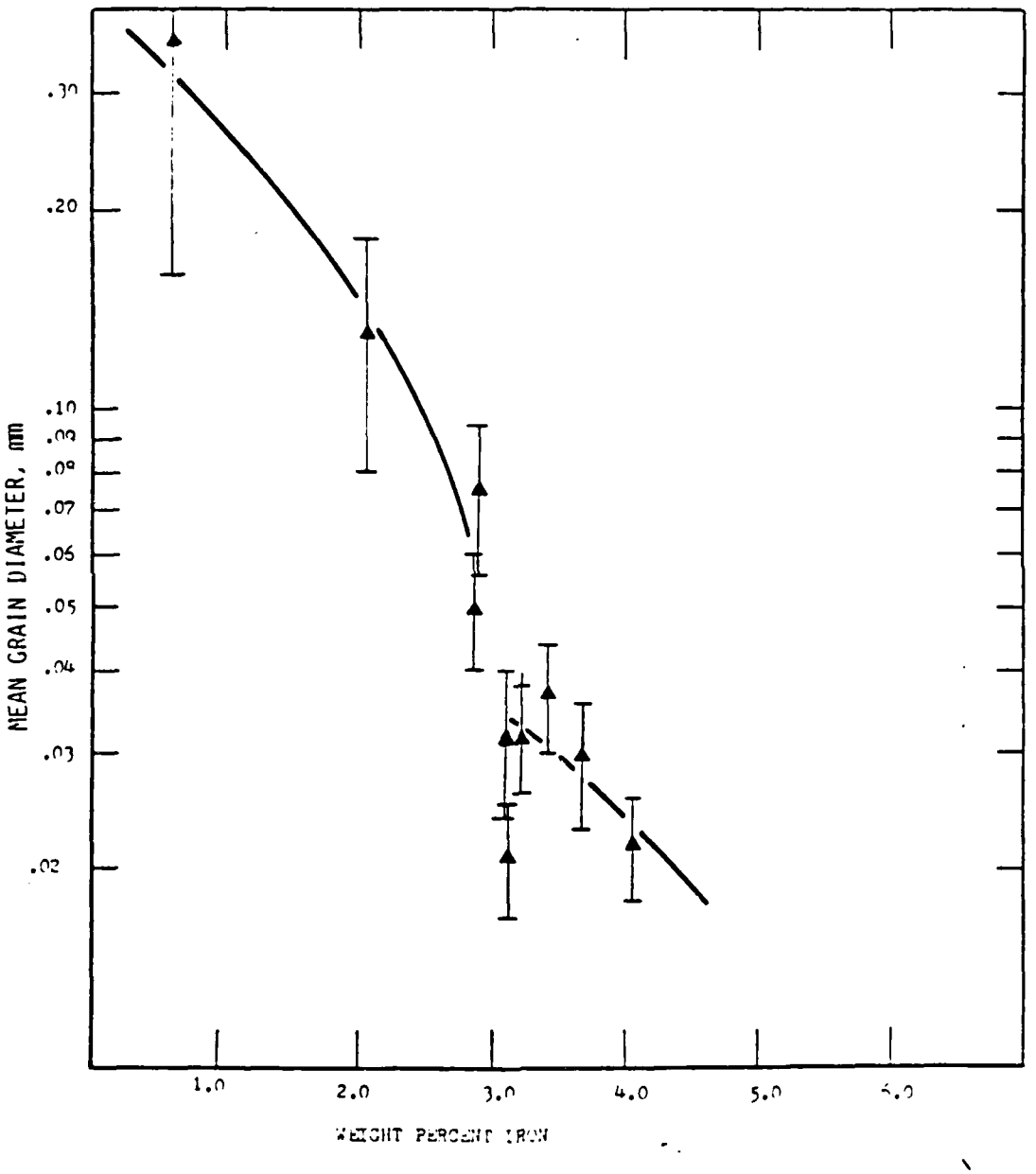

Figure 6. Mean grain size vs iron content for samples quenched in water from their liquidus.

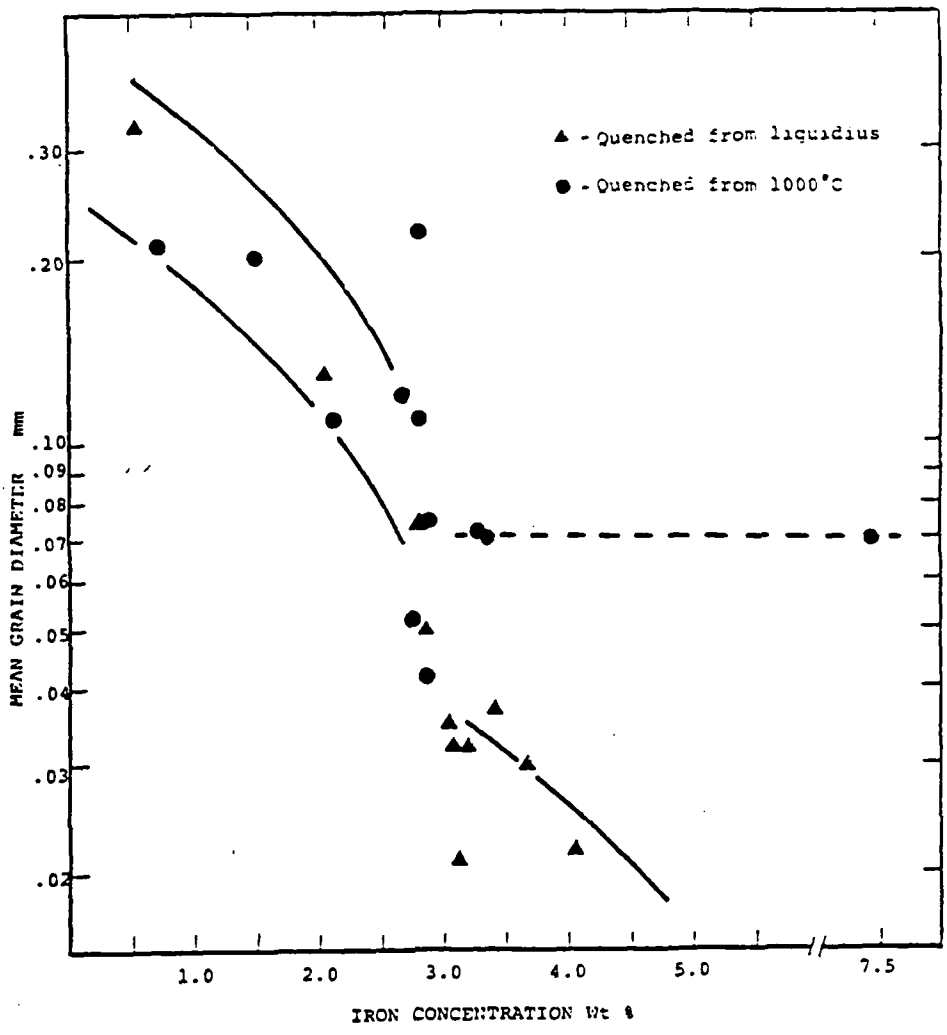

Figure 7. Grain size vs iron content--Comparison between water quenched and solidified while levitated samples.

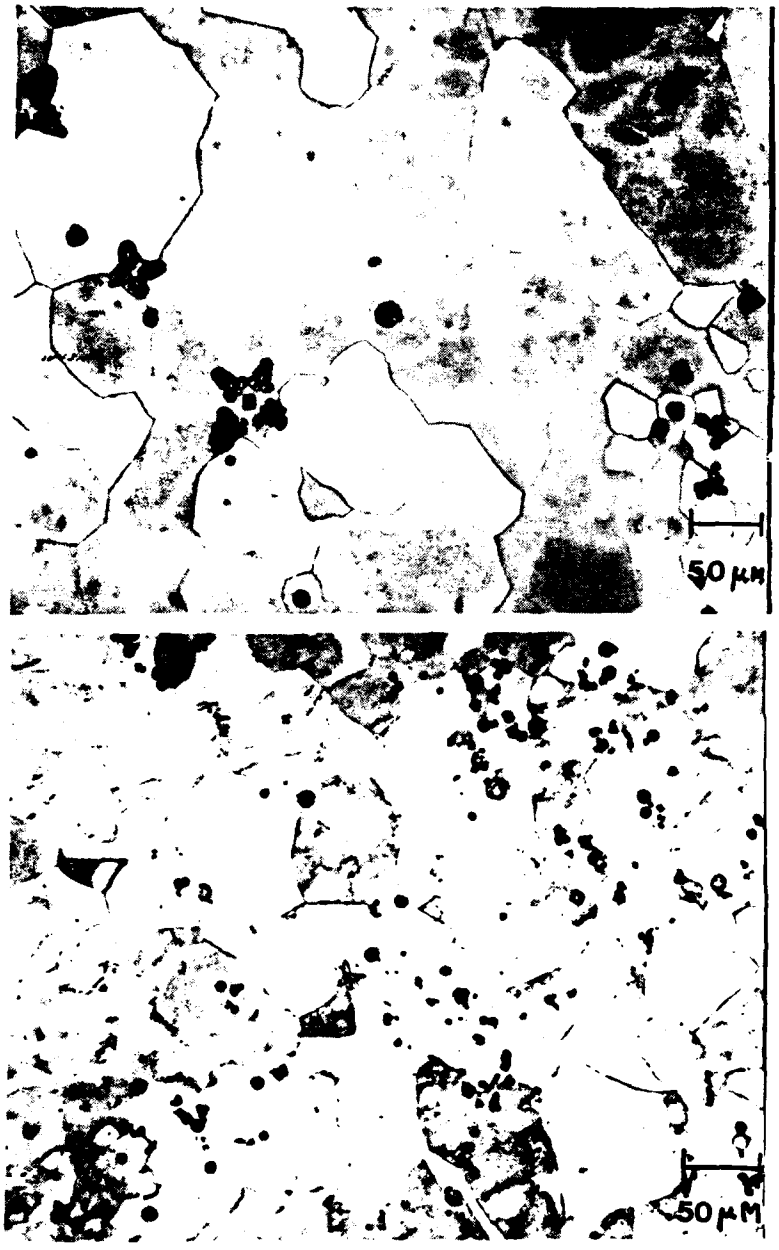

Figure 8. The microstructure of two samples with 2.8% Fe solidified in the levitated state--note the difference in the grain size.

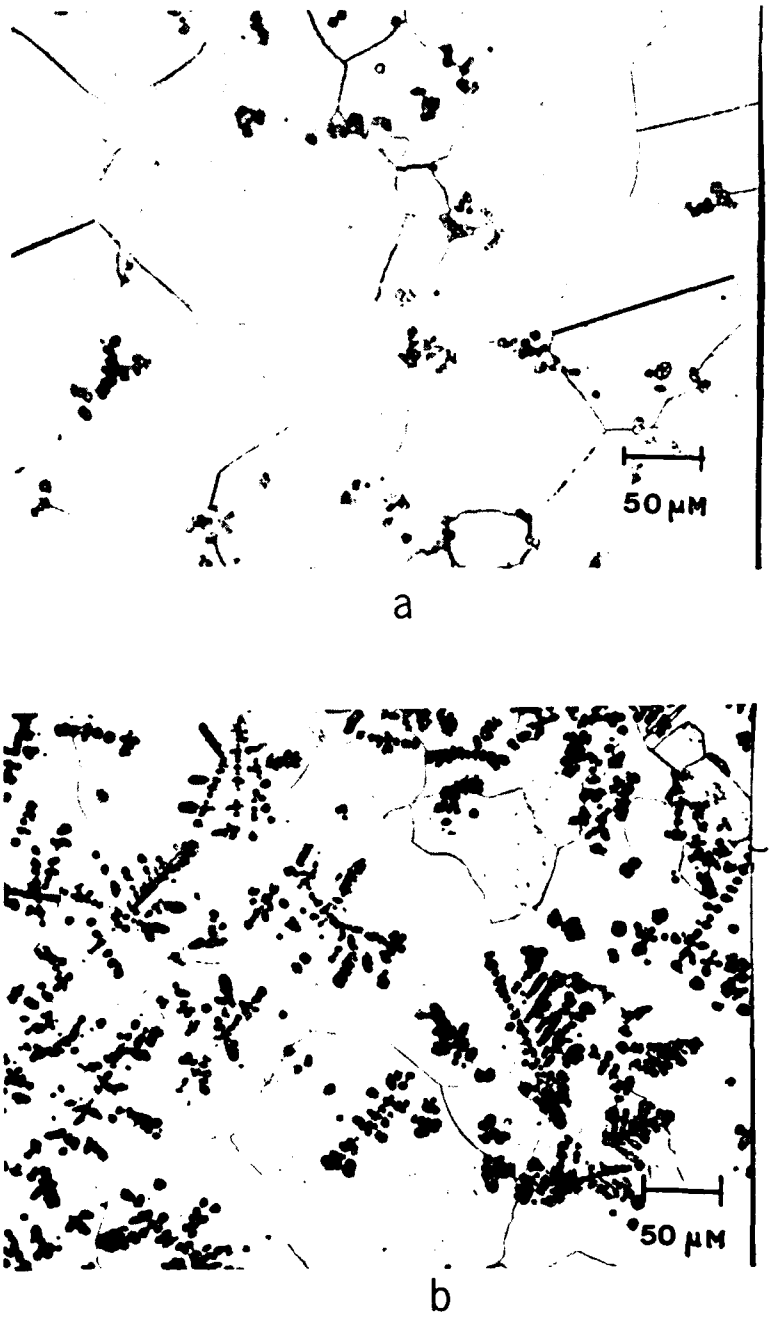

Figure 9. The grain size of two hyperperitectic alloys solidified in the levitated state: (a) 3.27 and (b) 7.46 % Fe.

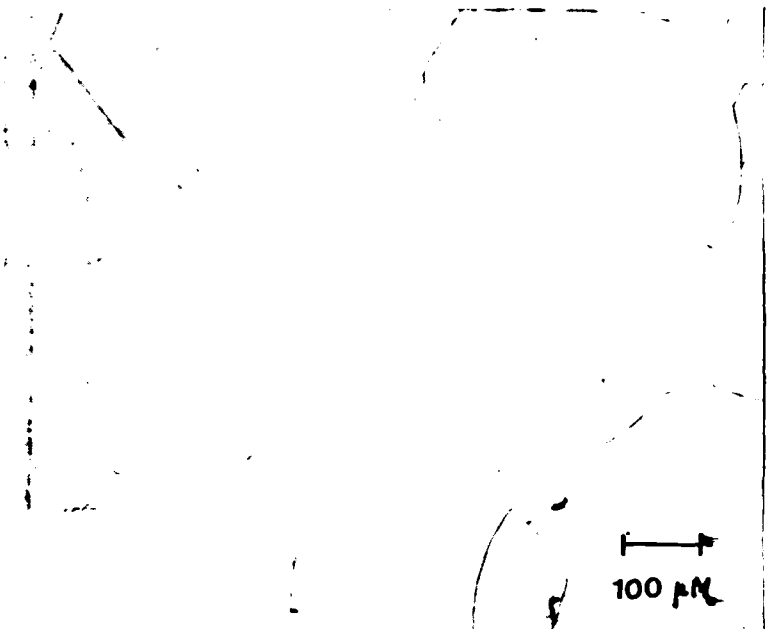

a

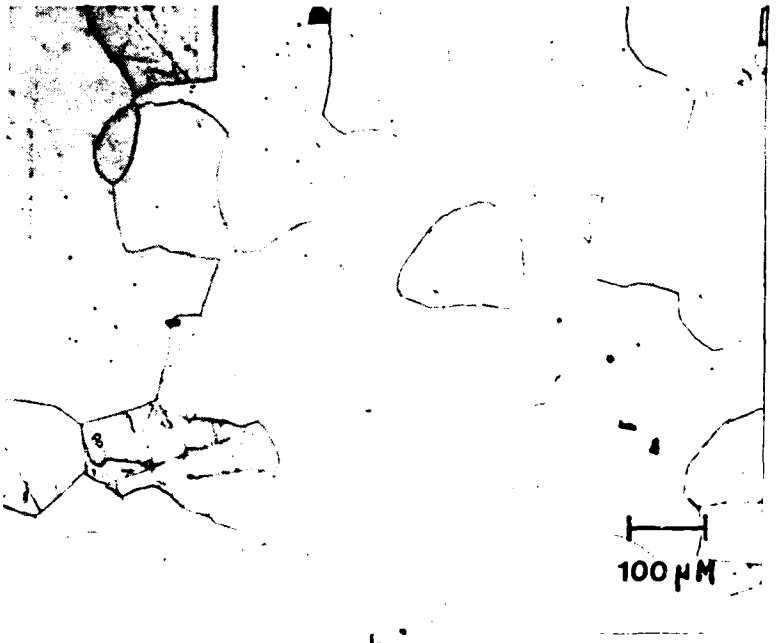

b

Figure 10. Effect of iron on the grain size of two hypoperitectic alloys quenched from liquidus: (a) 0.57 and (b) 2.05 % Fe.

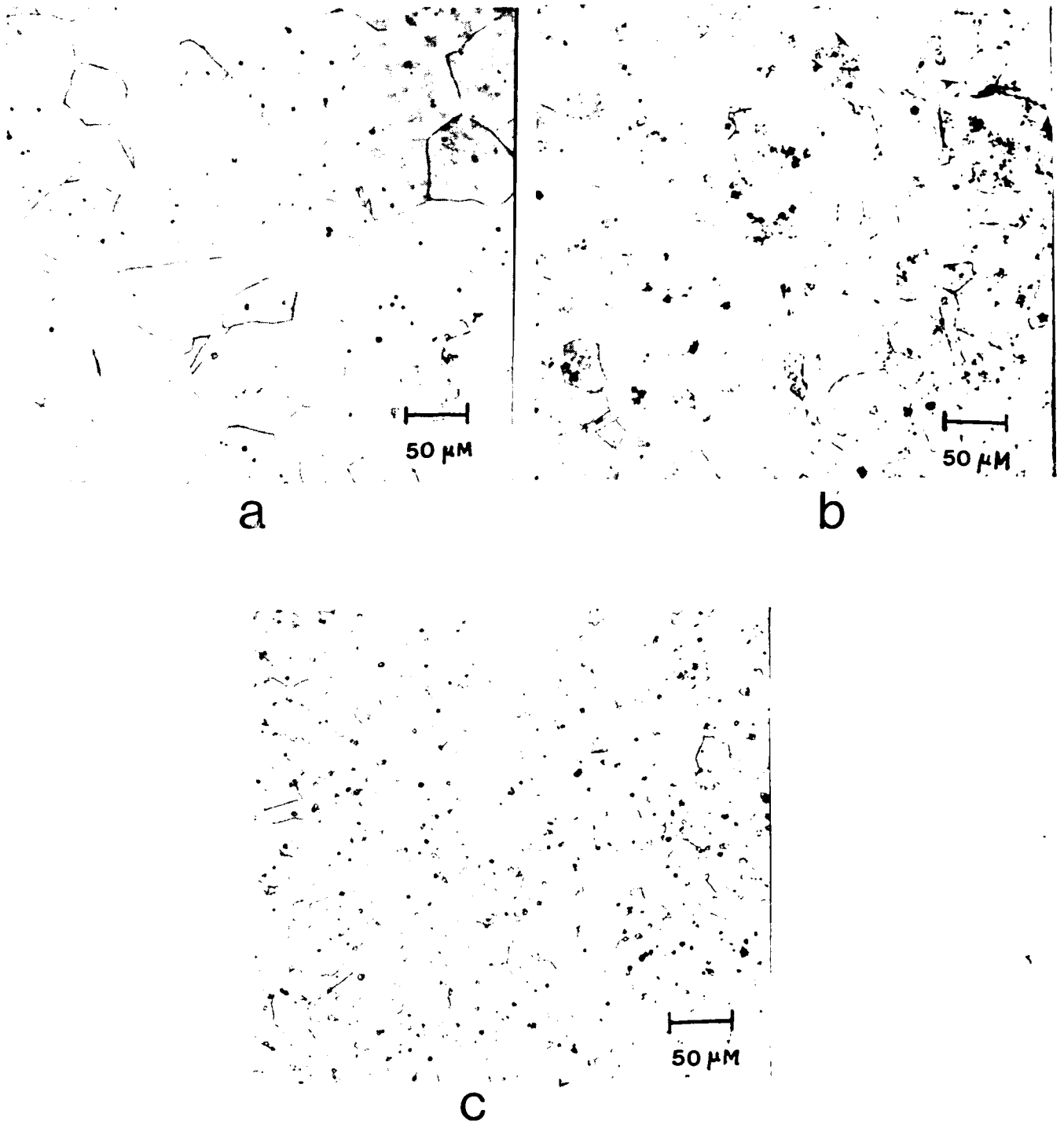

Figure 11. Effect at iron additions on the grain size of copper in hyperperitectic alloys quenched from their liquidus: (a) 2.84, (b) 3.12 and (c) 4.06 % Fe.

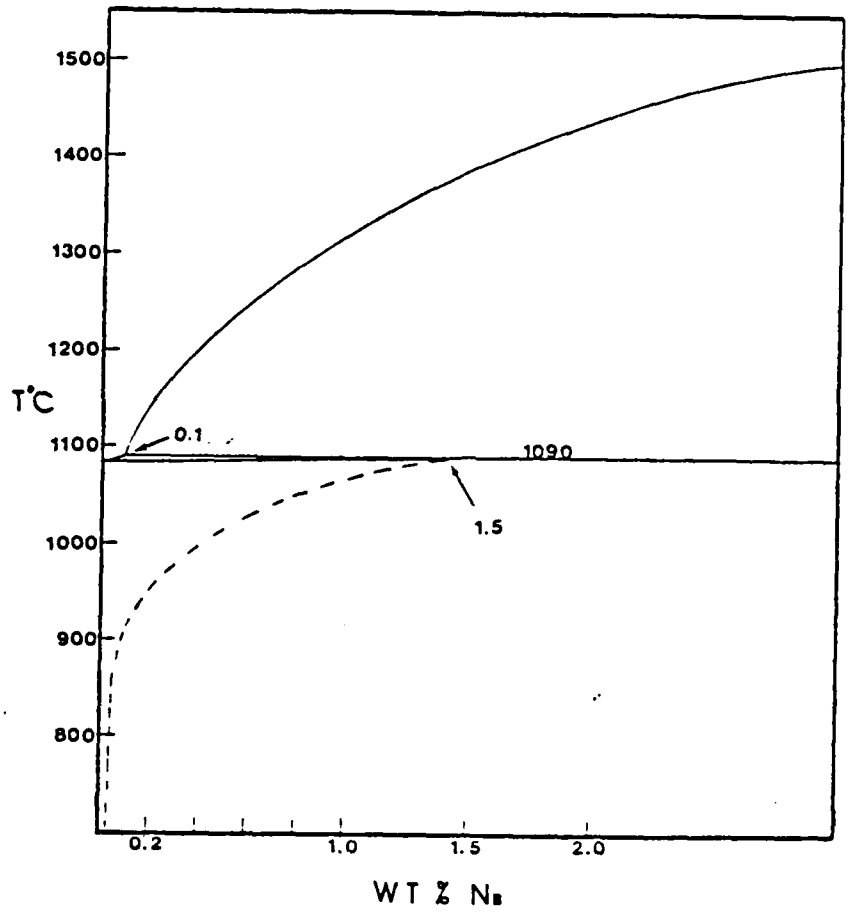

Figure 12. The Copper-Niobium phase diagram on the copper rich side. (From Ref. 25).

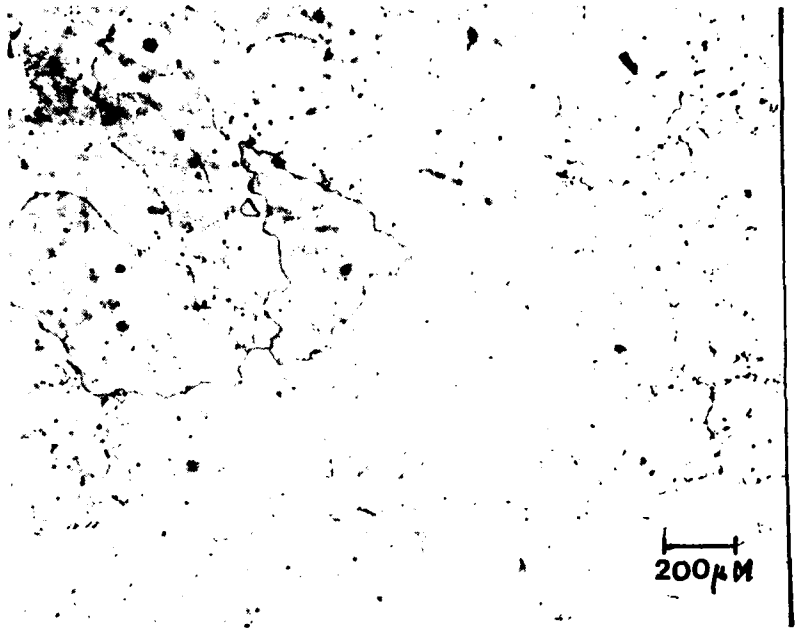

Figure 13. Microstructure of a Cu- 0.47 % Nb alloy quenched from the liquidus.

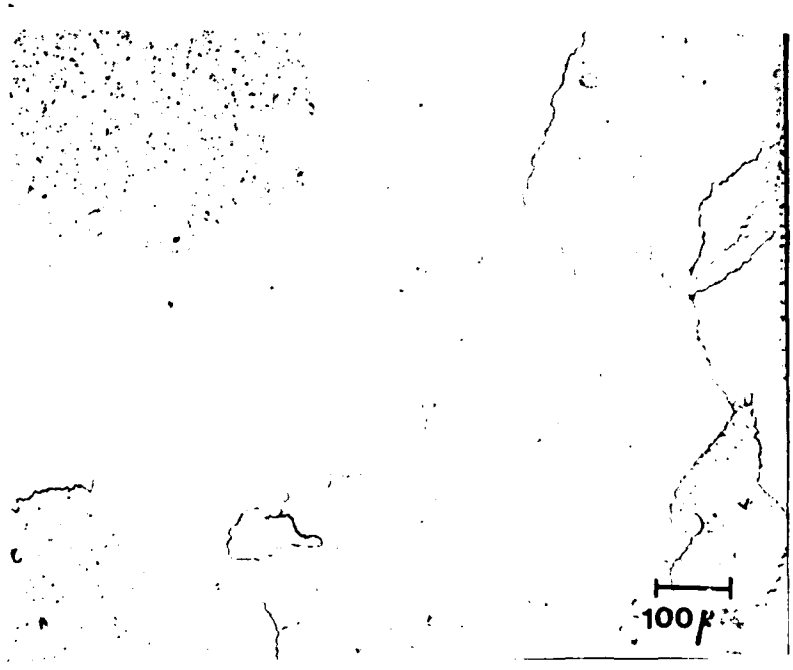

Figure 14. Microstructure of a Cu- 0.44 % Nb alloy quenched from 1000°C.

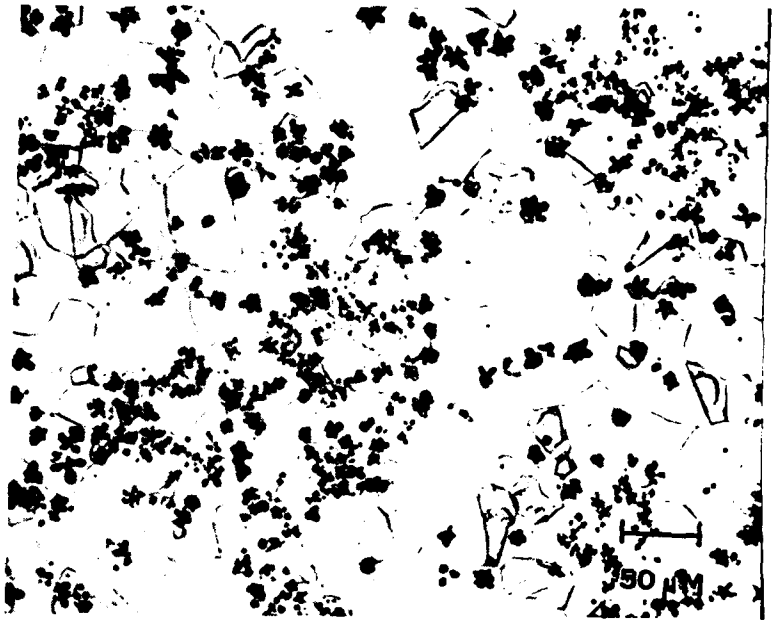

Figure 15. Microstructure of a Cu- 5.18% Nb alloy quenched from the liquidus; levitated in the presence of hydrogen.

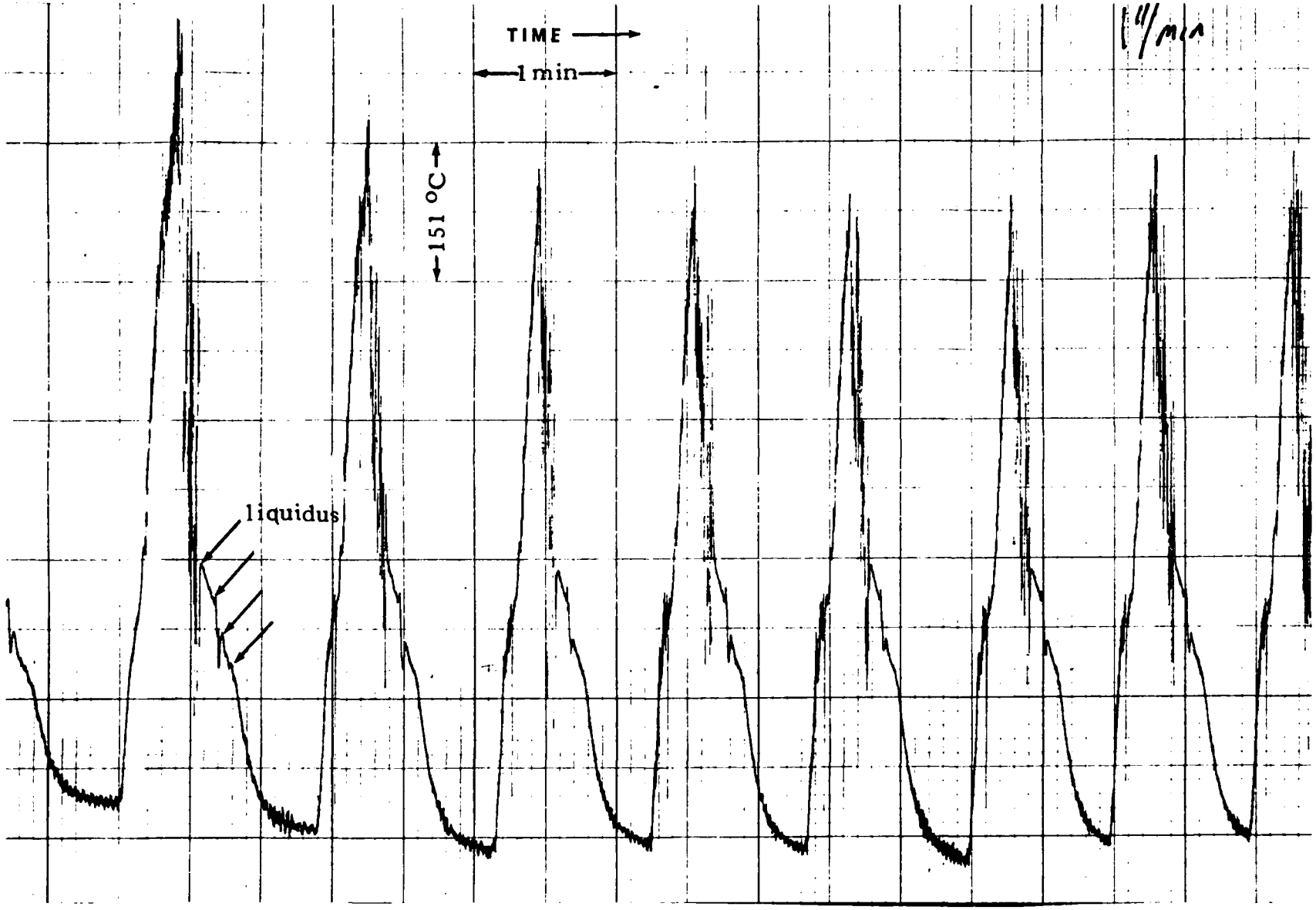

Figure 16. Heating and cooling cycles for a 60 Cr-40 Ni sample, showing various thermal arrests.

a

b

Figure 17. Structure of a 70 Cr-30 Ni sample quenched at 1400°C in water--note the formation of the peritectic phase around the primary dendrites: magnification (a) 100X, and (b) 1000X.

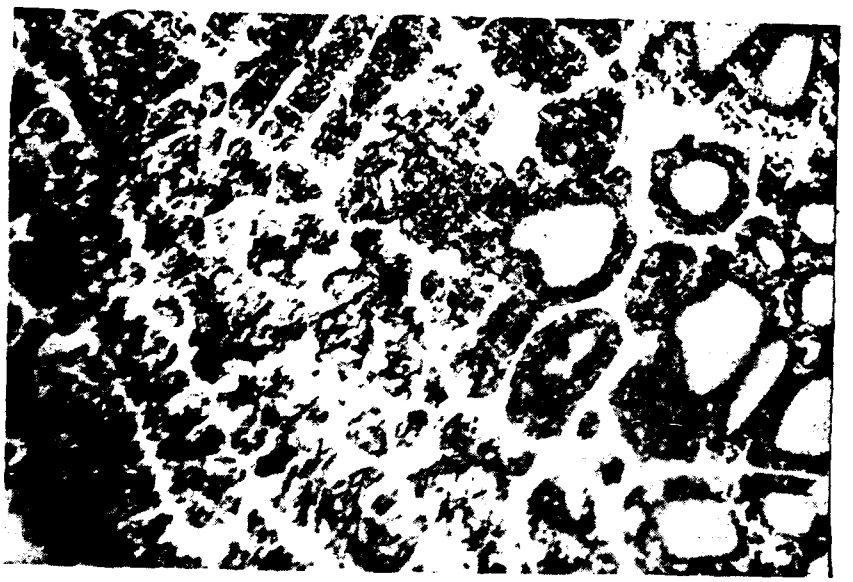

a

b

Figure 18. Structure of a 70 Cr-30 Ni sample quenched at 1400°C in water--note solid state reactions occurring in the peritectic phase. Magnification: (a) 500X, and (b) 1000X.

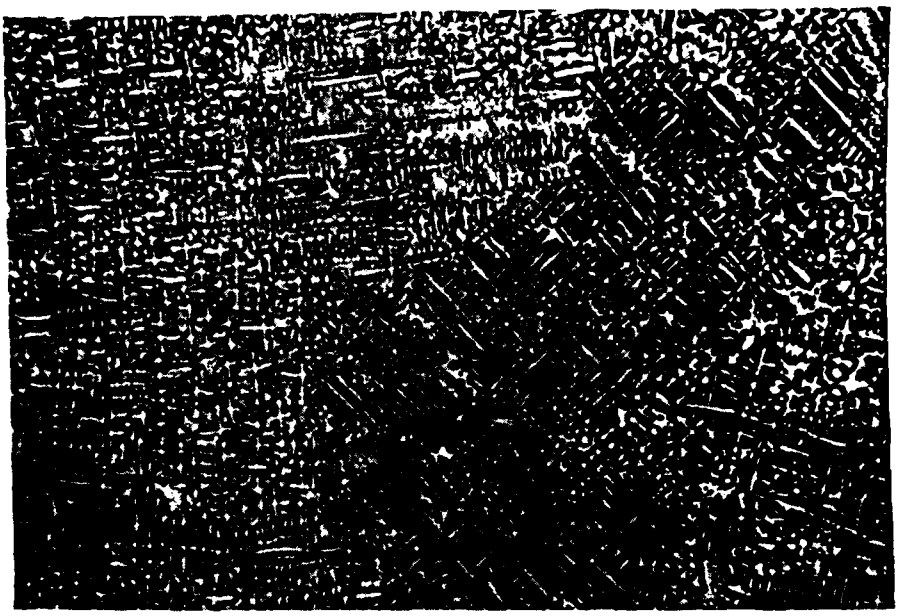

a

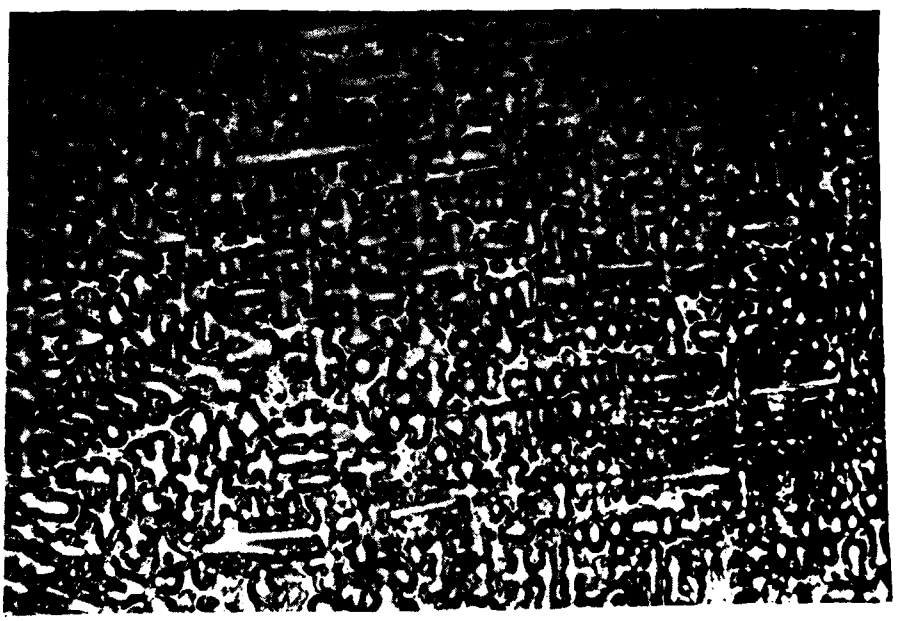

b

Figure 19. Structure of a 70 Cr-30 Ni sample solidified while levitated and quenched at 908°C: magnification (a) 50X and (b) 100X.

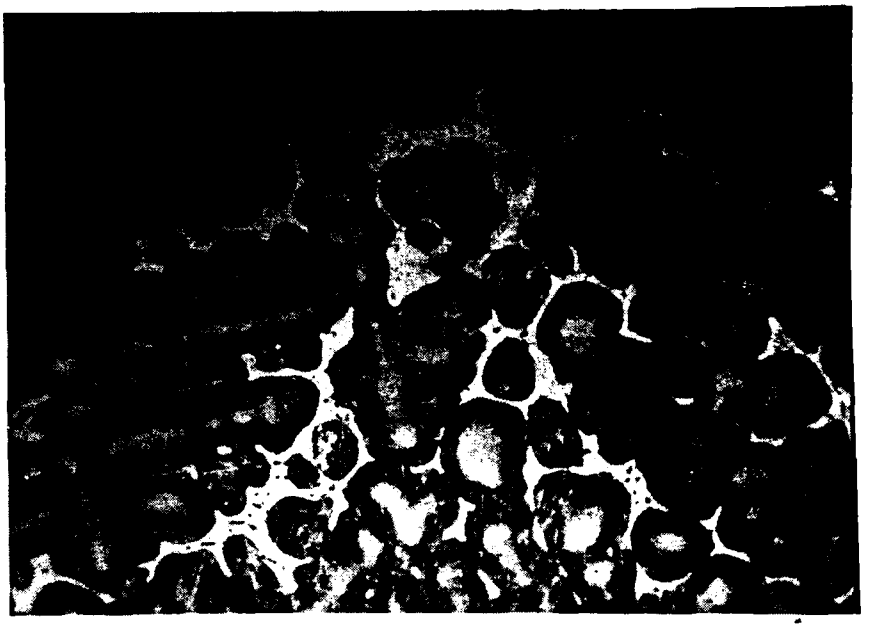

a

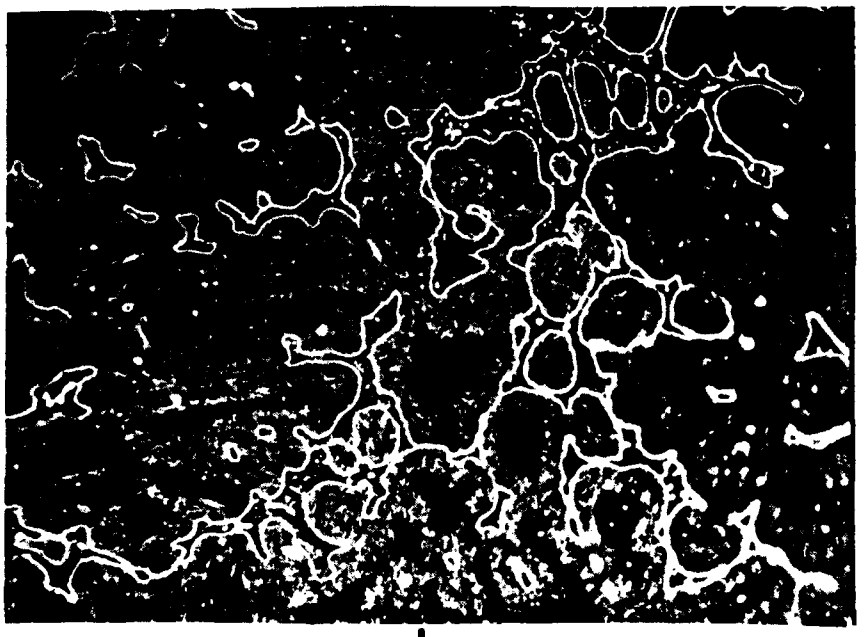

b

Figure 20. Structure of a 70 Cr-30 Ni sample quenched at 908°C, showing solid state transformation in the peritectic phase: (a) bright field, and (b) dark field. Magnification 200X.

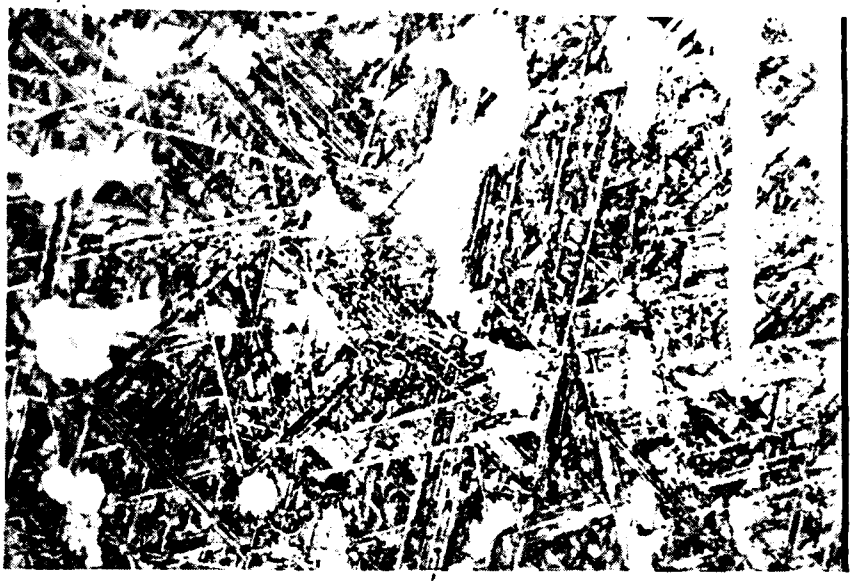

a

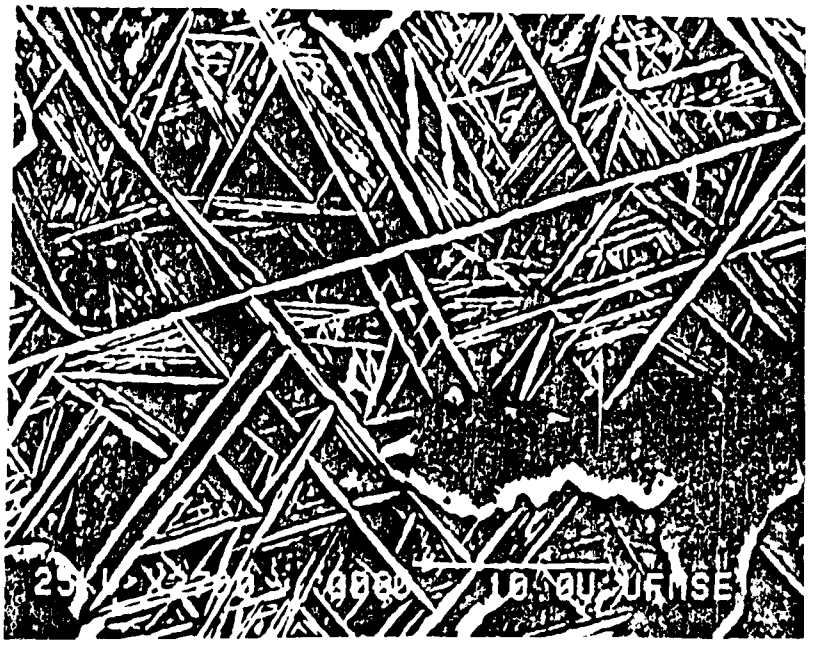

b

Figure 21. Widmanstätten plates in a 60 Cr-40 Ni alloy quenched at 870°C: (a) optical micrograph at magnification 1000X, and (b) SEM photograph at 2700X.

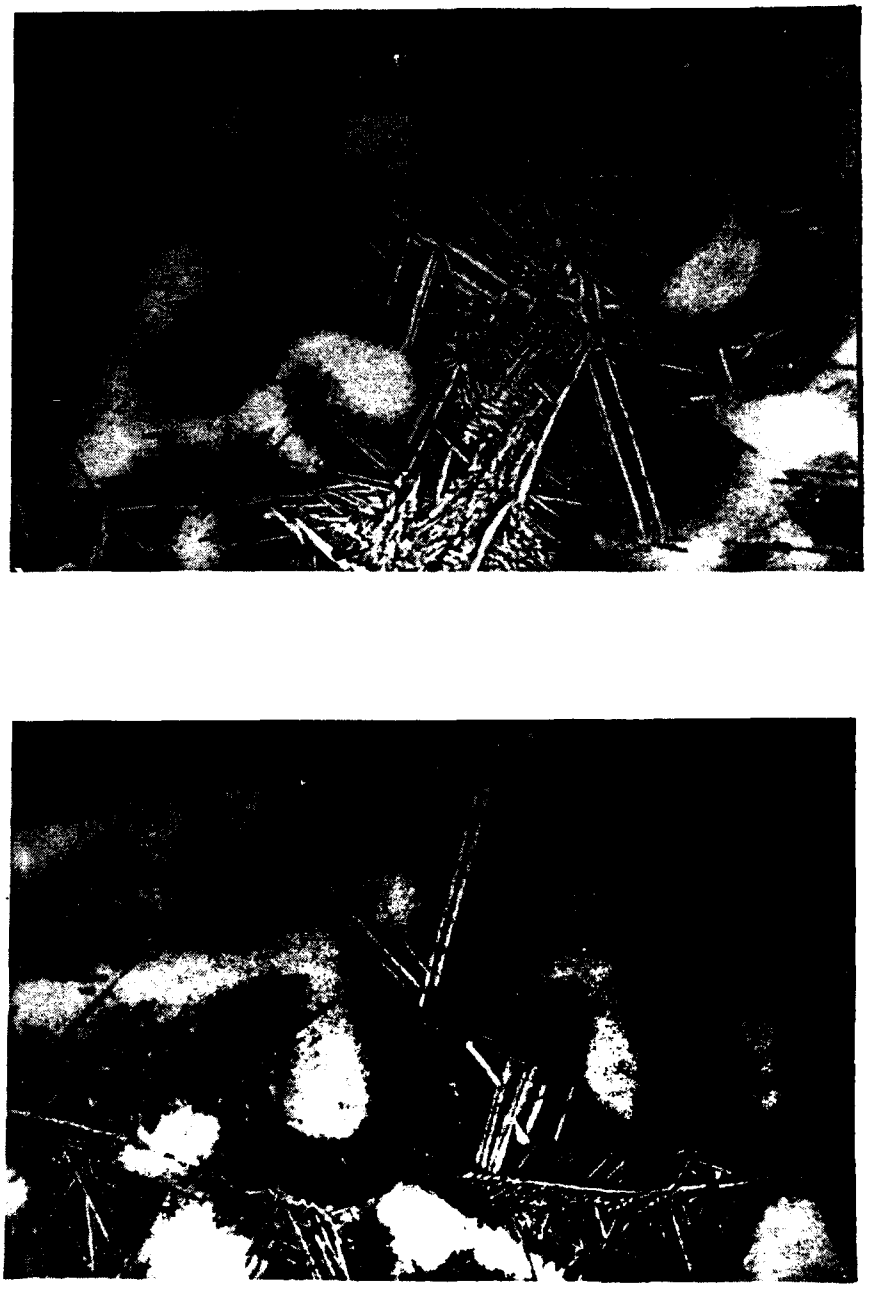

Figure 22. Structure of a 65 Cr-35 Ni sample quenched at 1412°C, showing basket-weave type morphology. Magnification 1000X.

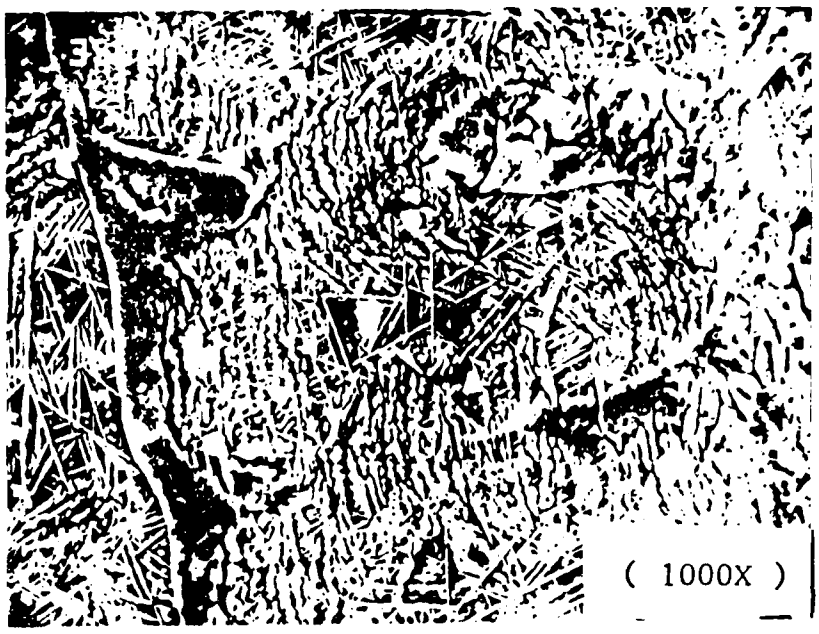

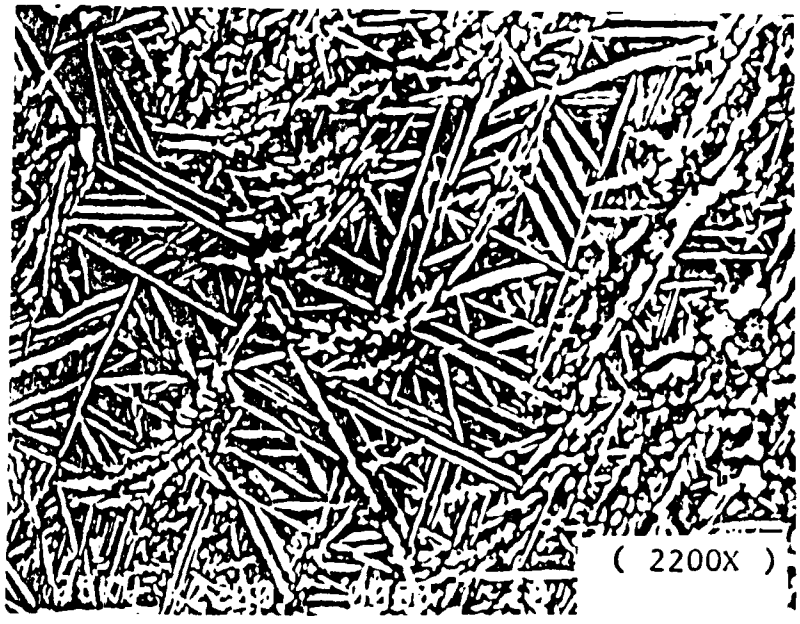

Figure 23. Widmanstätten plates and blocky type morphology in a 60 Cr-40 Ni sample quenched at 870°C.

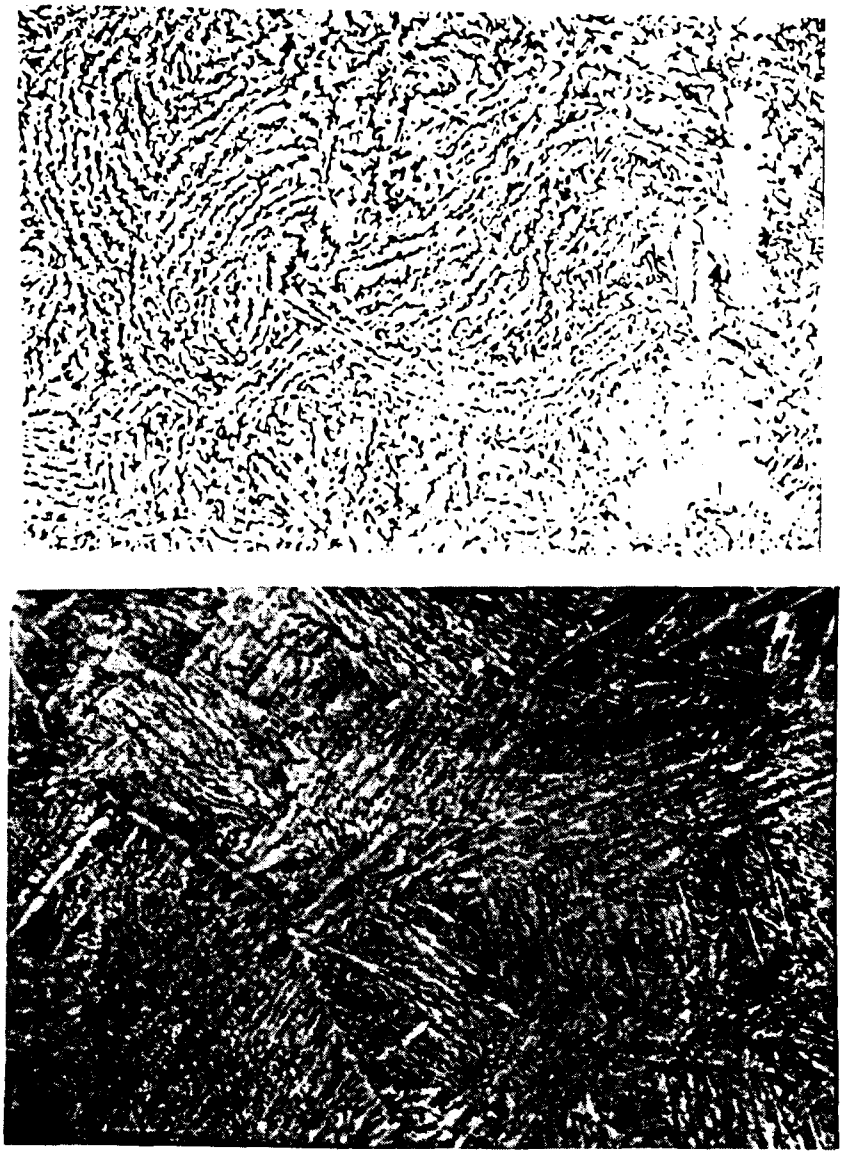

Figure 24. Lamellar morphology in a 60 Cr-40 Ni sample quenched at 870°C. Magnification 1000X.

Figure 25. Structure of a 60 Cr-40 Ni sample quenched in water from the liquidus. Magnificatioin 100X.

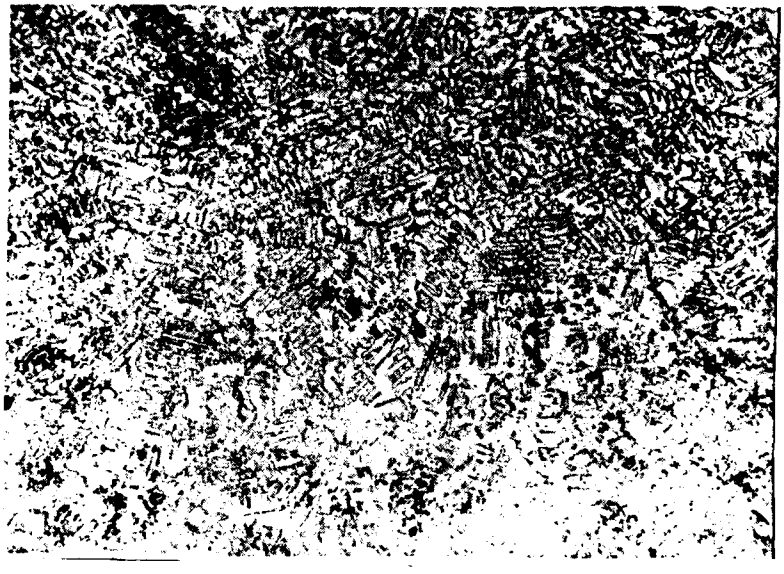

Figure 26. Structure of a 60 Cr-40 Ni sample quenched from solid plus liquid region. Magnification 100X.

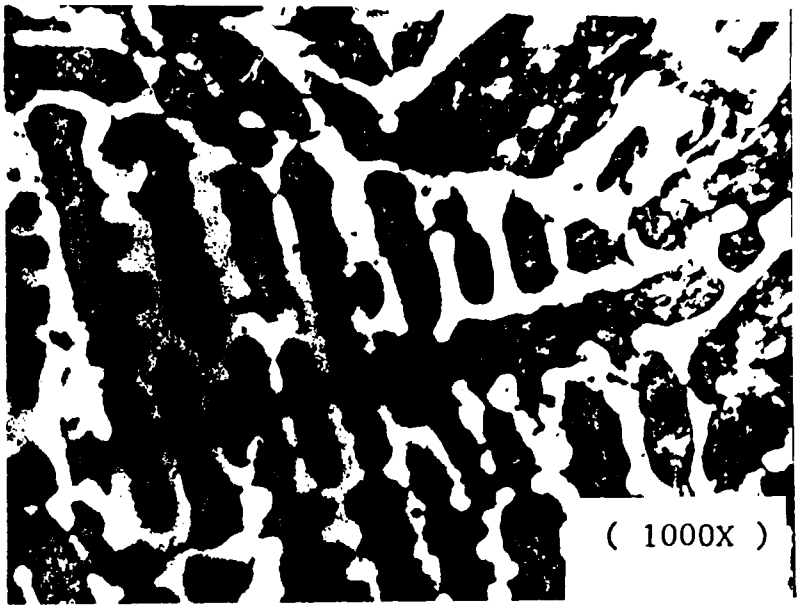

Figure 27. Structure of the sample shown in Figure 26, but at a higher magnification.

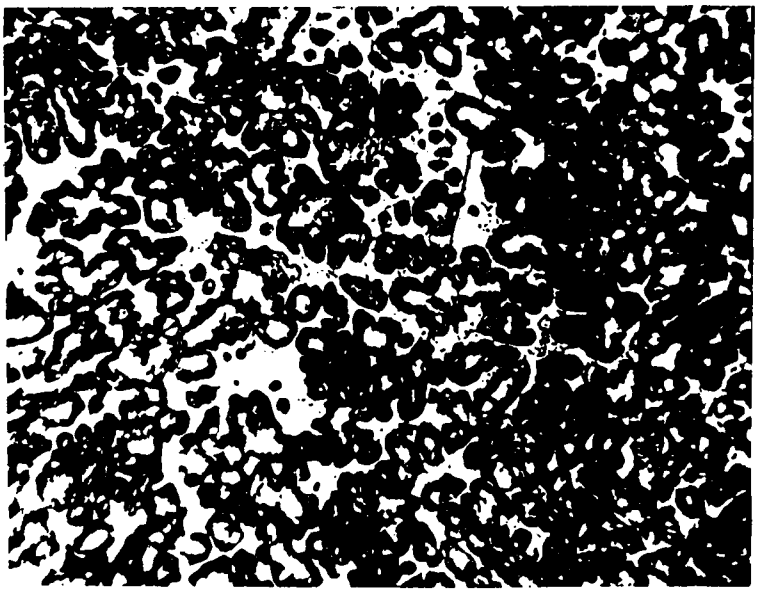

Figure 28. Structure of a 60 Cr-40 Ni solidified in the levitated state then quenched. Magnification 250X.

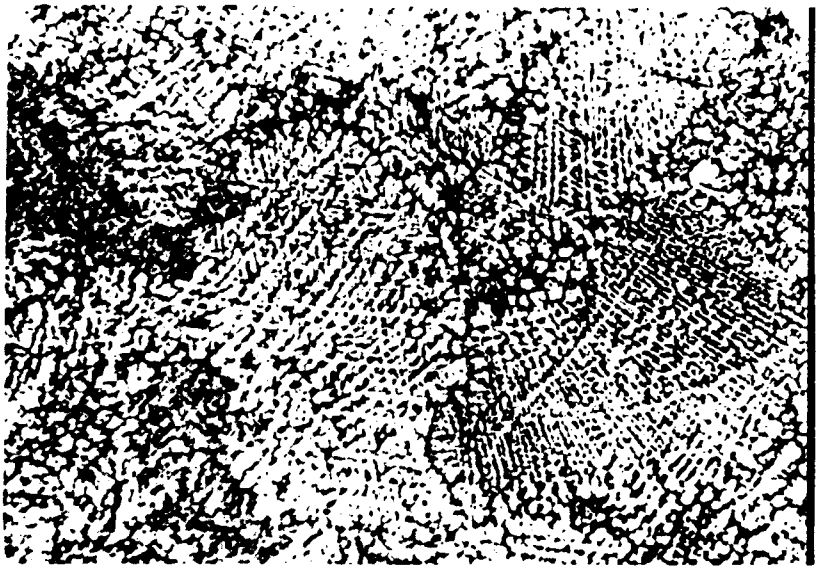

Figure 29. Structure of an 80 Cr-20 Ni sample in water from the liquidus. Magnification 175X.

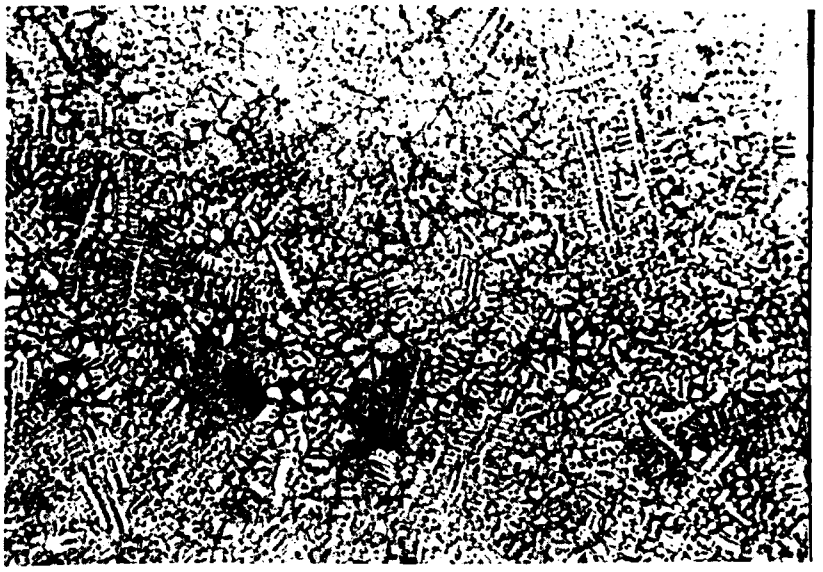

Figure 30. Structure of an 80 Cr-20 Ni sample solidified in the levitated state. Magnification 175X.

END

FILMED

1-85

DTIC